Article

TRANSPARENT PROCESS

THE EMBO JOURNAL

The GTPase Rab39a promotes phagosome maturation into MHC-I antigen-presenting compartments

Freidrich M Cruz, Jeff D Colbert & Kenneth L Rock*

Abstract

For CD8 T lymphocytes to mount responses to cancer and virally-infected cells, dendritic cells must capture antigens present in tissues and display them as peptides bound to MHC-I molecules. This is most often accomplished through a pathway called antigen cross-presentation (XPT). Here, we report that the vesicular trafficking protein Rab39a is needed for optimal cross-presentation by dendritic cells *in vitro* and cross-priming of CD8 T cells *in vivo*. Without Rab39a, MHC-I presentation of intraphagosomal peptides is inhibited, indicating that Rab39a converts phagosomes into peptide-loading compartments. In this process, Rab39a promotes the delivery of MHC-I molecules from the endoplasmic reticulum (ER) to phagosomes, and increases the levels of peptide-empty MHC-I conformers that can be loaded with peptide in this compartment. Rab39a also increases the levels of Sec22b and NOX2, previously recognized to participate in cross-presentation, on phagosomes, thereby filling in a missing link into how phagosomes mature into cross-presenting vesicles.

Keywords cross-presentation; dendritic cells; endosomal trafficking; phagosomes; Rab39a

Subject Categories Immunology; Membranes & Trafficking

DOI 10.15252/embj.2019102020 | Received 17 March 2019 | Revised 4 November 2019 | Accepted 12 November 2019 | Published online 10 December 2019

The EMBO Journal (2020) 39: e102020

Introduction

Most cells display on their MHC-I molecules peptides that are exclusively derived from their expressed genes (Cruz *et al*, 2017). In this process, cytosolic and nuclear proteins are hydrolyzed into oligopeptides by proteasomes (Rock *et al*, 1994) and a fraction of the resulting peptides are translocated by the transporter of antigen presentation (TAP) into the endoplasmic reticulum (ER) (Neefjes *et al*, 1993). In this location, peptides of the correct length and sequence bind to MHC-I molecules, and these complexes are then released and transported to the cell surface. This antigen presentation mechanism allows CD8 effector T cells to identify and eliminate cells that are synthesizing abnormal proteins, e.g., from viruses or mutations. In contrast, extracellular antigens are not presented on MHC-I molecules because they fail to gain access to the cytosol (Moore *et al*, 1988). The exception to this rule occurs in certain professional antigen-presenting cells (APC), such as macrophages and particularly dendritic cells (DCs), which can acquire exogenous antigens and present them on MHC-I molecules through a process called cross-presentation (XPT) (Rock *et al*, 1990b; Grant & Rock, 1992; Shen *et al*, 1997). XPT plays a key role in the initiation of CD8 T cell responses to cancers and viral infections (Huang *et al*, 1994; Sigal *et al*, 1999). This is because to initiate a CD8 T cell response in a naïve host, DCs must acquire antigens from the tissues, migrate to secondary lymphoid tissues, and subsequently present peptides from the tissue antigens on MHC-I molecules to CD8 T cells (Jung *et al*, 2002; Hildner *et al*, 2008).

Antigens internalized by phagocytosis are cross-presented 10^3–10^4-fold more efficiently than ones acquired by fluid-phase endocytosis (Kovacsovics-Bankowski *et al*, 1993; Pfeifer *et al*, 1993; Harding & Song, 1994). Therefore, phagosomes are key entry points for cross-presented antigens, especially particulate ones, such as dying cells and cell debris. Once antigens are in phagosomes, the major mechanism for XPT is often the phagosome-to-cytosol (P2C) pathway (Kovacsovics-Bankowski & Rock, 1995). In this pathway, some of the internalized antigen is transferred to the cytosol, where it is then degraded by proteasomes, and a fraction of the resulting antigenic peptides are subsequently transported to MHC-I molecules by the TAP transporter.

Proteomic analysis of phagosomes revealed that these vacuoles contained some components that are normally resident in the ER, such as Sec61 and TAP (Houde *et al*, 2003; Trost *et al*, 2009; Campbell-Valois *et al*, 2012). These molecules from the ER potentially provide mechanisms in phagosomes to export antigen to the cytosol (via endoplasmic reticulum associated degradation, ERAD), as well as to import proteasome-derived peptides back into phagosomes (via TAP) for binding to MHC-I molecules (a "phagosome-to-cytosol-to-phagosome" (P2C2P) pathway) (Ackerman *et al*, 2003, 2006; Zehner *et al*, 2015; Lawand *et al*, 2016). However, there are many unresolved questions about the mechanisms of delivery and role of ER components in phagosomes, including whether and to

Department of Pathology, University of Massachusetts Medical School, Worcester, MA, USA
*Corresponding author. Tel: +1 508 856 2521; E-mail: kenneth.rock@umassmed.edu

what extent a P2C2P mechanism and intraphagosomal MHC-I peptide-loading actually contributes to XPT.

One unresolved issue is how ER components are delivered to phagosomes. It is thought that some ER components are selectively transported to phagosomes, but how this occurs is incompletely understood (Guermonprez *et al*, 2003; Campbell-Valois *et al*, 2012). Vesicular transport is often directed by Rab proteins, but whether these trafficking proteins underlie the delivery of ER components for XPT is unknown. Ultimately, SNARE proteins allow transport vesicles to fuse with target membranes, and the SNARE protein Sec22b has been implicated in the final delivery to phagosomes of some ER components, including a P2C protein transport mechanism and TAP (Cebrian *et al*, 2011). There is evidence that Sec22b promotes XPT (Cebrian *et al*, 2011; Alloatti *et al*, 2017) but this role has been questioned (Wu *et al*, 2017).

Other related and unresolved issues regarding the P2C2P pathway is whether and if so how MHC-I molecules are transported to and loaded with peptides in phagosomes. A role for Sec22b in the delivery of MHC-I molecules to phagosomes has not been reported. The MHC-I molecules that are released from the ER have bound peptides and are transported to the cell surface. Such complexes can be internalized from the plasma membrane into phagosomes (Lizee *et al*, 2003; Basha *et al*, 2008) or transported to these vacuoles from a recycling compartment after Toll-like receptor (TLR) stimulation (Nair-Gupta *et al*, 2014). However, once peptides are bound to MHC-I molecules, they are not readily exchanged for new ones and it is therefore unclear how peptide-occupied MHC-I molecules could acquire new cross-presented peptides in phagosomes. Peptide-empty MHC-I (open conformers), which can load with peptides, are unstable and retained in the ER (Ljunggren *et al*, 1990). Whether these unstable complexes can escape the ER retention mechanisms, remain intact during transport and/or survive in the acidic-catabolic environment of phagolysosome until they are loaded with peptide are unclear.

With these issues in mind, we identified Rab39a in an unbiased forward genetic screen as a gene of interest that contributed to XPT in DCs. Here, we investigate the role of Rab39a and find that it is a missing link in this process that promotes the delivery of components from the ER-Golgi to phagosomes and converts these vacuoles into peptide-loading compartments for empty MHC-I molecules.

Results

Rab39a in dendritic cells is required for optimal XPT

To investigate the role of Rab39a in XPT, we transfected the DC line DC3.2R with siRNA against Rab39a, which resulted in a substantial reduction in Rab39a mRNA (Fig 1A). The cells were then incubated with various forms of exogenous Ova, all of which were presented by the P2C pathway of XPT (Kovacsovics-Bankowski & Rock, 1995; Shen *et al*, 2004), and an H2-K^b—SIINFEKL specific reporter CD8$^+$ T cell line (RF33-Luc). RF33-Luc is stably transfected with an NFAT-luciferase construct and expresses luciferase in proportion to the strength of T cell receptor stimulation. As shown in Fig 1B, silencing of Rab39a reduced XPT of Ova-conjugated iron oxide particles (henceforth called Ova-Fe) as compared to the negative control (silencing of the MHC-II gene H2 I-Ab). This inhibition was not as strong as that observed with the loss of β2M (~85% inhibition), but it was nevertheless substantial (~75% reduction). Silencing of Rab39a also reduced XPT of Ova-conjugated particles to latex beads (Ova-latex) (Fig 1C), as well as soluble Ova (Fig 1D). A similar inhibition of XPT was observed when Rab39a was silenced in another dendritic cell line, DC2.4, or in immortalized macrophages (IMMP) (Fig EV1A and B). We tested multiple independent siRNAs specific for different sequences in Rab39a and found that all of them inhibited XPT (Fig EV1C). In further related studies that will be described below, primary dendritic cells from a Rab39a knock out mouse also showed a reduction in XPT.

We also performed a reciprocal gain of function experiment wherein we examined the effect on XPT of selectively inducing the expression of Rab39a. For this experiment, and others below, we transduced a doxycycline (dox)-inducible hemagglutinin (HA)-tagged Rab39a construct into Rab39a-deficient DC3.2 cells (DC3.2-Rab39a). In this cell line, the endogenous Rab39a was knocked out using CRISPR/Cas9 system (Fig EV1D). This allowed us to reconstitute the expression of Rab39a upon addition of dox (Fig EV1E). Dox-induced expression of Rab39a increased XPT of Ova-Fe (Fig 1E) as well as Ova-latex (Fig EV1F).

To further explore the mechanism of Rab39a reconstitution, we also transduced Rab39a KO cells with GDP-locked (S22N) or GTP-locked (Q72L) mutants of Rab39a (Seto *et al*, 2011). Only the WT form of Rab39a was able to enhance XPT (Fig EV2A–C). Investigating further, we found that the GDP-locked form of Rab39a was unstable, and degraded in the cells unless proteasome activity was inhibited (Fig EV2D); therefore we could not distinguish whether the lack of reconstitution with this construct was due to inadequate levels versus functional inactivation of Rab39a. However, the GTP-locked construct was expressed but functionally inactive, which is consistent with what has been observed with some other Rab proteins (Weigert *et al*, 2004; van Weering *et al*, 2007). These data suggest that GTP hydrolysis is important in conferring proper function of Rab39a.

In summary, loss of function and gain of function experiments gave concordant results, which together establish a role for Rab39a in XPT.

Rab39a functions selectively in XPT

Next, we investigated the role of Rab39a in other antigen-presenting pathways in DCs. We first examined whether the loss of Rab39a affected the presentation on MHC-II molecules of the same exogenous antigens by the same DC. To do this, siRNA experiments were performed as described above and the DCs then were co-cultured with reporter CD4$^+$ T cells (MF2-Luc) which are specific for I-A^b- Ova$_{258–276}$ complexes. In these experiments, the β2M siRNA became the negative control and the H2-I-Ab siRNA was the positive control. While silencing I-A^b gene expression inhibited MHC-II antigen presentation as expected, treatment of the cells with Rab39a siRNA did not reduce MHC-II presentation for Ova-Fe (Fig 2A), Ova-latex (Appendix Fig S1A), or soluble Ova (Appendix Fig S1B). Rab39a knockdown did not affect Class II presentation across the entire antigen dose–response curve, including at limiting doses of antigen.

We also examined whether dox-induced Rab39a expression, which increased XPT as described above, had any effect on MHC-II

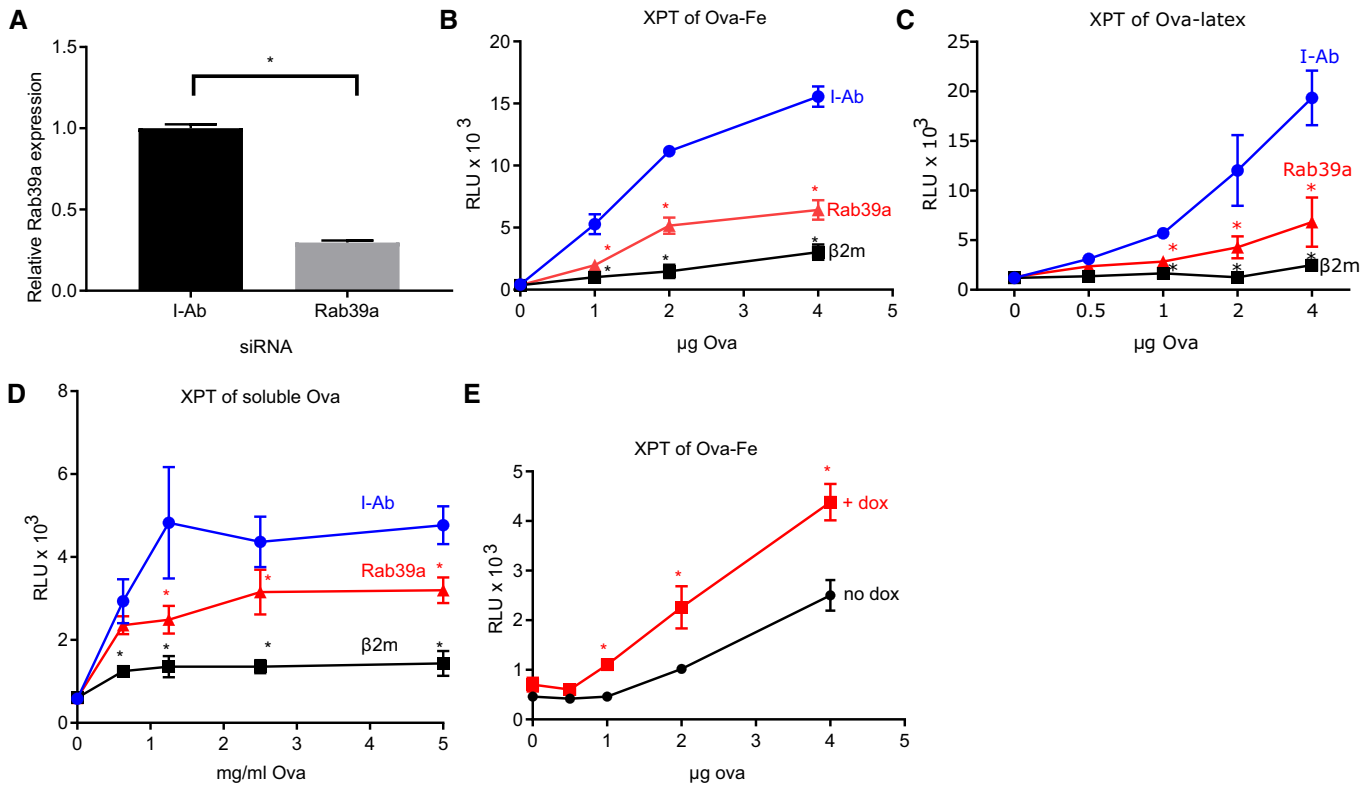

Figure 1. Rab39a in dendritic cells is required for optimal cross-presentation.

A Relative expression of Rab39a in siRNA-treated cells after 48 h of knockdown. Rab39a expression in I-Ab or Rab39a siRNA-treated cells was normalized to expression in cells treated with control β2m siRNA. Error bars show SD between three independent experiments. *$P \leq 0.05$ using two-way Student's *t*-test.

B–D XPT of siRNA-treated DC3.2R cells after 48 h of knockdown. Treated cells were fed with the indicated amounts of Ova-Fe (B), Ova-latex (C), or unconjugated soluble Ova (D). The cells were then exposed to RF33.70-Luc Reporter CD8 T cells overnight. RLU indicates relative luminescence units produced by reporter T cell stimulation. Error bars show SD of ≥ 3 replicate wells. *$P \leq 0.05$ versus control I-Ab using two-way ANOVA. Representative plot of three independent experiments.

E DC3.2-Rab39a cells (Rab39a KO with dox-inducible Rab39a) were incubated overnight with or without 1 μg/ml dox to induce Rab39a expression. About 1×10^5 cells were then fed with Ova-Fe and exposed to reporter T cells as in (B). Error bars show SD of duplicate wells. *$P \leq 0.05$ using two-way ANOVA. Representative plot of three independent experiments.

presentation. This gain of function experiment showed no significant effect on MHC-II presentation of Ova-Fe (Fig 2B).

The P2C pathway of XPT is thought to share a number of molecular components (e.g., MHC-I, proteasomes and TAP, etc.) with the Classical MHC-I presentation pathway. Therefore, we next investigated whether Rab39a played a role in the presentation of peptides from endogenously expressed antigens that were presented by the Classical MHC-I pathway. For this analysis, we generated a DC line that could inducibly express a cytosolic form of Ova (DC3.2 NS-Ova) upon addition of dox. MHC-I presentation of this form of antigen requires hydrolysis by proteasomes, after which the resulting peptides are imported into the ER through TAP, trimmed by ERAP1, and loaded onto MHC-I molecules for transport to the surface (Neefjes *et al*, 1993; Rock *et al*, 1994; Serwold *et al*, 2002; York *et al*, 2002). We also generated a second DC line (DC3.2 Ub-S8L) that in the presence of dox expressed the SIINFEKL (S8L) peptide conjugated to the C-terminus of ubiquitin (York *et al*, 2006). Upon expression of this construct, deubiquitinases in the cell liberated the S8L peptide, thereby bypassing the need for proteasomal processing and peptidase trimming (Bachmair *et al*, 1986; Rock *et al*, 1994). The S8L peptide, however, still required transport through TAP and loading onto MHC-I molecules in the ER. In these experiments, varying amounts of endogenous antigen expression were induced with a titration of dox. Silencing of Rab39a in these dendritic cell lines did not inhibit MHC-I presentation of S8L from either the cytosolic Ova or ubiquitin-S8L constructs, even under limiting conditions (Fig 2C and D). In contrast, silencing β2M blocked the presentation from the endogenous constructs, as expected.

We also looked at the effect of silencing Rab39a on surface MHC-I levels by flow cytometric analysis. This analysis was of interest because peptide-binding is required for MHC-I molecules to exit the ER and therefore a reduction in peptide supply reduces MHC-I levels on the cell surface. In addition, defects in MHC-I trafficking from the ER to the plasma membrane would be detected in this assay. The silencing of Rab39a did not reduce cell surface levels of MHC-I H-2K^b (or of I-A^b) (Fig 2E). In contrast, silencing β2M markedly decreased the surface expression of MHC-I, as expected. Rescue of Rab39a in DC3.2-Rab39a cells also did not change surface MHC-I and MHC-II levels (Appendix Fig S1C).

These data indicated that Rab39a expression selectively affected XPT. The findings that Rab39a was not affecting any of the steps in the Classical MHC-I pathway, including ones in the cytosol, ER, or

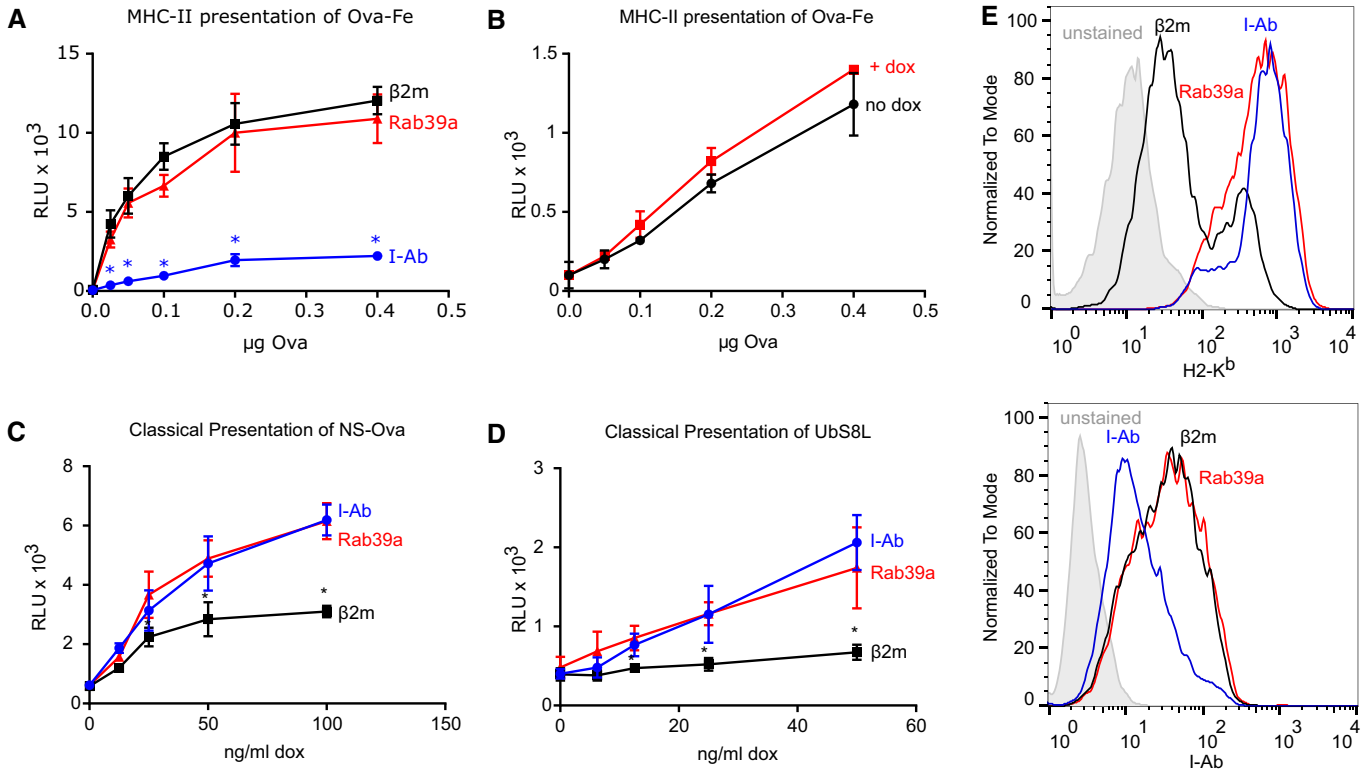

Figure 2. Rab39a functions selectively in XPT.

A MHC-II presentation of siRNA-treated DC3.2R cells after 48 h of knockdown. Treated cells were fed with the indicated amounts of Ova-Fe. The cells were then exposed to MF2.2D9-Luc Reporter CD4 T cells overnight. Error bars show SD of ≥ 3 replicate wells. *$P \leq 0.05$ versus negative control β2m using two-way ANOVA. None of the bead concentrations is $P \leq 0.05$ for Rab39a siRNA versus β2m. Representative plot of three independent experiments.

B DC3.2-Rab39a cells (Rab39a KO with dox-inducible Rab39a) were incubated overnight with or without 1 µg/ml dox to induce Rab39a expression. About 1×10^5 cells were then fed with Ova-Fe and exposed to reporter T cells as in (A). Error bars show SD of duplicate wells. None of the bead concentrations is $P \leq 0.05$ for Rab39a siRNA versus β2m using two-way ANOVA. Representative plot of three independent experiments.

C, D MHC-I presentation of SIINFEKL-H2-K^b complexes on siRNA-treated DC3.2 NS-Ova (C) or DC3.2 UbS8L (D) cells. Forty-eight hours after siRNA transfection, the indicated amount of dox was added to the cells to induce Ova expression. After 2 h at 37°C, RF33.70-Luc CD8 T cells were added along with Brefeldin A (Golgiplug) to a final concentration of 1:1,000. The cells were incubated overnight for reporter T cell luciferase expression. Error bars show SD of ≥ 3 replicate wells. *$P \leq 0.05$ versus negative control I-Ab using two-way ANOVA. None of the dox concentrations is $P \leq 0.05$ for Rab39a siRNA versus I-Ab. Representative plot of three independent experiments.

E Flow cytometric analysis of surface H2-K^b and I-A^b levels of siRNA-treated DC3.2R cells. Shown are results after 48 h of knockdown. Representative plot of three independent experiments.

involved in transit and display on the cell surface, strongly suggested that Rab39a was playing its role in XPT somewhere in or around phagosomes. Because of this, and Rab39a's published endosomal localization (Seto *et al*, 2011, 2013), we next focused on evaluating how Rab39a affected the phagosomal processes that occur during XPT.

Rab39a localization and function in endosomes and phagosomes of DCs

The initial step in XPT is antigen capture and internalization into DCs. It was previously reported that Rab39a was involved in endocytosis (Chen *et al*, 2003). However, our findings that loss of Rab39a only affected DC XPT, but not MHC-II presentation of the same antigen, strongly argued that the inhibition of XPT was not due to reduced antigen uptake. To further analyze this issue, we measured the effect of Rab39a on the phagocytosis of latex particles by flow cytometry. The loss of Rab39a, or its dox-induced expression, did not affect either the number of DCs ingesting beads or the overall fluorescence intensity (which equates to the number of beads per DC) and therefore had no effect on phagocytosis (Fig 3A and B). In contrast, addition of cytochalasin D, which disrupts microfilaments needed for phagocytosis, completely inhibited the internalization of beads, as expected. These results are consistent with our findings that Rab39a had no effect on MHC-II presentation of the bead-bound antigens (which also require phagocytosis). Therefore, Rab39a is not exerting its effects on XPT at the level of antigen internalization.

To analyze the subcellular localization of Rab39a, DC3.2-Rab39a were incubated with dox, permeabilized, and stained for HA and known endosomal markers. We were unable to image endogenous Rab39a, due to a lack of suitable antibodies, thus we obtained the results using Rab39a fusion proteins. Rab39a colocalized with both Rab7 (Fig EV3A) and Lamp2 (Fig 3C), which are two markers of

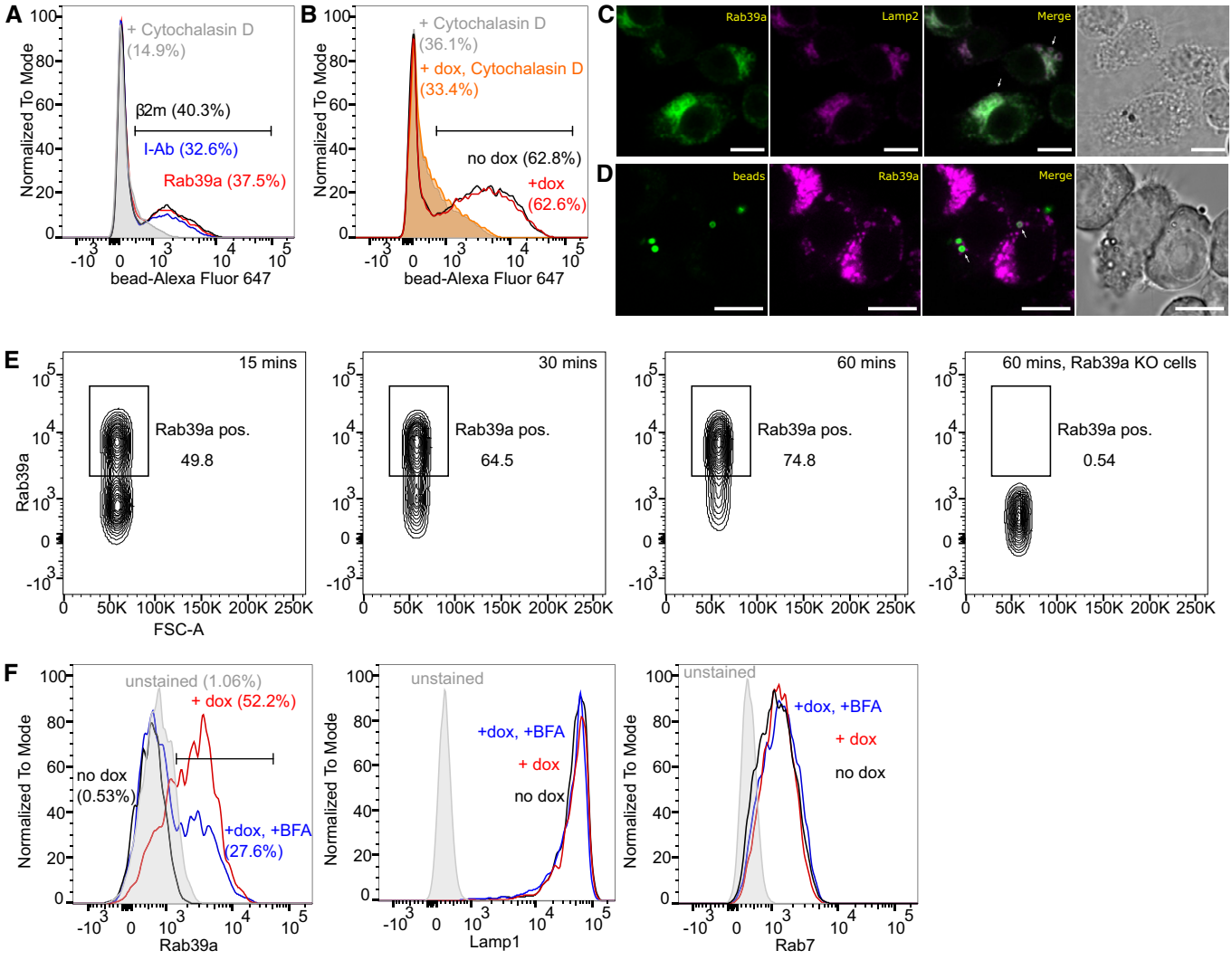

Figure 3. Rab39a localization and function in endosomes and phagosomes of DCs.

A Phagocytosis assay after 48 h of siRNA knockdown. DC3.2R cells treated with the indicated siRNAs were incubated on ice for 30 min with 4 beads per cell of Alexa-Fluor 647 conjugated beads. The mixture was then placed in media at 37°C for 1 h. Cells were harvested and incubated on ice with 1 mg/ml of trypan blue to quench uneaten beads before analysis through flow cytometry. As a control, some cells were incubated with 10 μM cytochalasin D during the feeding period. Shown are percentages of cells that have taken up beads. Representative plot of two independent experiments.

B Rab39a was induced in DC3.2-Rab39a cells (Rab39a KO with dox-inducible Rab39a) via overnight incubation with 1 μg/ml dox. KO and rescued cells were then harvested and assayed as in (A) for phagocytosis. Representative plot of two independent experiments.

C DC3.2-Rab39a cells were induced to express Rab39a overnight. Cells on coverslips were washed, fixed, and stained according to the listed protocol and antibodies. Green = Rab39a (HA-tag), Magenta = Lamp2. Arrows highlight punctate structures with colocalization. Scale bar = 10 μm. Representative image of two independent experiments.

D DC3.2 Rab39a KO cells were transduced with dox-inducible mcherry-tagged Rab39a. Cells were plated in 35 mm glass bottom dishes and induced with 1 μg/ml dox. The next day, 1-μm latex beads conjugated with Alexa 488-NHS (1 bead/cell) were added. After 2 h at 37°C, cells were imaged under a Leica TCS SP5 confocal microscope. Green = Alexa 488 labeled beads. Magenta = mcherry-Rab39a. Arrows highlight internalized beads surrounded by Rab39a. Scale bar = 10 μm. Representative image of two independent experiments.

E About 5×10^5 of DC3.2-Rab39a cells were induced to express Rab39a overnight with 1 μg/ml dox in a 6-well plate. Cells were fed at 1 bead/cell of biotinylated 6-μm magnetic beads for the indicated lengths of time. Magnetic bead phagosomes were isolated using the listed protocol. Phagosomes were washed and stained for Rab39a (HA-tag). Representative data for three independent experiments are presented.

F About 1.25×10^5 of DC3.2-Rab39a cells were incubated in a 12-well plate overnight ± dox (1 μg/ml) to induce Rab39a. Cells were fed at 4 beads/cell of biotinylated-Ova 6-μm magnetic beads for 3 h with or without 1:1,000 BFA (Golgiplug, BD). Phagosomes were isolated using the listed protocol. Isolated phagosomes were washed, permeabilized, and stained. Shown are histograms of indicated stains as well as % of Rab39a-positive phagosomes. Representative plot of two independent experiments is presented.

late endosomes. We also imaged a Rab39a-mcherry fusion in living DC3.2 cells and observed that this construct was localized in punctate vesicles. When these cells were fed overnight with lysosensor dextran (which fluoresces at 521 nm when in acidic conditions), Rab39a could be seen surrounding dextran that was fluorescing (Fig EV3B). The terminal destination of endocytosed dextrans is

Lamp1-positive and Rab7-positive compartments (Humphries *et al*, 2011). Thus, Rab39a localized with acidic, late endosomal compartments in live cells; this is a similar subcellular distribution as has been reported for Rab39a in other cell types (Seto *et al*, 2013; Gambarte Tudela *et al*, 2015).

We also analyzed by confocal microscopy Rab39a-mcherry expressing DC3.2 cells that had been incubated with latex beads and observed that this Rab protein was recruited to phagosomes (Fig 3D). To further examine the kinetics of this process and quantify the number of Rab39a positive vacuoles, we incubated DC3.2-Rab39a with beads for various lengths of time, purified their phagosomes, and quantified the amount of HA in intact phagosomes by flow cytometry (Figs 3E and EV3C). Rab39a was detected in a subset of phagosomes (~50%) at the earliest time point measured (15 min) and the percentage of these positive phagosomes progressively increased at later time points (30 and 60 min); at 60 min, ~75% of phagosomes were Rab39a positive. The signal was specific as no staining was observed when the cells did not express Rab39a. Both WT and GTP-locked forms of Rab39a were able to localize to phagosomes while the GDP-locked form was undetectable (because, as noted above, it is unstable) (Fig EV3D–F).

Previous reports have shown that in certain cell types, Rab39a localized to the Golgi compartment (Chen *et al*, 2003; Mori *et al*, 2013) and that Rab39a regulated autophagy (Seto *et al*, 2013). Because of these findings, we thought it might be possible that Rab39a was shuttling vesicles from the ER-Golgi to the phagosome. To investigate the origin of Rab39a on phagosomes, we tested the effect of BFA, an agent that blocks all transport out of the ER-Golgi. We found that if dox-induced DC3.2-Rab39a cells were incubated with beads in the presence of BFA, Rab39a failed to reach many phagosomes (Fig 3F). In contrast, BFA did not prevent phagosomes from acquiring Rab7 and Lamp1, both of which are classic markers of phagosome maturation. Although Lamp 1 originates from the ER-Golgi, BFA did not acutely affect its delivery to phagosomes presumably because Lamp1 has a long half-life (> 30 h) (Krzewski *et al*, 2013) and is acquired from preexisting peripheral pools, e.g., from lysosomes that fuse with the phagosome. Therefore, Rab39a is recruited to phagosomes from the ER-Golgi and this process is independent of at least some of the events in phagosome maturation.

Silencing Rab39a affects the ability of phagosomes to generate peptide–Class I complexes

As noted above, the mechanism of XPT underlying the antigens in our system is the P2C pathway. In this pathway, antigens in the phagosome are transferred to the cytosol, where they are hydrolyzed into oligopeptides by proteasomes and then in most circumstances transported by the transporter of antigen presentation (TAP) to MHC-I molecules originally thought to be in the ER (Kovacsovics-Bankowski & Rock, 1995). However, TAP is not only resident in the endoplasmic reticulum (ER) and but is also found on phagosomes. Published data have raised the possibility that TAP translocates peptides from the cytosol into phagosomes for binding to intraphagosomal MHC-I molecules (Ackerman *et al*, 2003). Since we mapped the function of Rab39a to phagosomes, we sought to determine whether this GTPase might be affecting the generation of peptide-MHC complexes in these vacuoles. To test this possibility, we assayed whether loss of Rab39a affected the XPT of mature antigenic peptides (ones that are the correct size to bind to MHC-I and therefore do not need any cleavage by proteasome) that were targeted into phagosomes. To perform this experiment, the peptide CIINFEKL was conjugated to magnetic beads via a disulfide bond to the peptides N-terminal cysteine residue. CIINFEKL is a cysteine containing variant of the Ova peptide SIINFEKL that is still recognized by our reporter RF33.70-Luc cells. The rationale for using these constructs was that they would be internalized into phagosomes, wherein the reducing environment of phagosomes (Singh & Cresswell, 2010) would release the mature peptide epitope. Once liberated, the peptide would be available to bind to MHC-I molecules present in the phagosomes (with no need for transport out of or back into phagosomes).

When we incubated Rab39a siRNA-treated cells with CIINFEKL beads, we observed that even with this form of antigen, silencing of Rab39a inhibited XPT (Fig 4A and B). Conversely, inducing Rab39a in DC3.2-Rab39a increased XPT from these peptide beads (Fig 4C). Furthermore, while the XPT of full-length Ova protein was TAP-dependent, the XPT of the intraphagosomal peptide was TAP-independent (Fig 4A and B), indicating that the CIINFEKL was almost certainly being loaded onto MHC-I within the phagosomes themselves. To determine whether similar results would be obtained with a second peptide, we synthesized CSNENMETM, a cysteine containing variant peptide of the influenza NP peptide ASNENMETM, which is presented on H2-D^b. The XPT of CSNENMETM was also Rab39a-dependent (Fig 4D). These data generalized our findings to two different antigens and two different MHC-I molecules. The data indicate that one of the ways that Rab39a is contributing to XPT is by promoting the generation of peptide-MHC-I complexes in the phagosome. This led us to further examine how Rab39a was influencing phagosomes.

Effect of Rab39a on intraphagosomal MHC-I molecules

Our findings that showed that Rab39a was required for the optimal XPT of antigens (CIINFEKL and CSNENMETM), which require neither transport to/from the cytosol nor proteolysis, led us to hypothesize that Rab39a might increase the amount of peptide-receptive MHC-I in phagosomes. To study this, we transduced DC3.2-Rab39a with H2-L^d, a MHC-I allele not present in our DC3.2 cells (henceforth called DC3.2-Rab39a-H2-L^d). H2-L^d is a useful tool for studying peptide-MHC-I loading because it is the only MHC-I molecule for which there are antibodies that specifically recognized peptide empty forms (64-3-7 antibody) or peptide-occupied forms (30-5-7s antibody) of this Class I molecule (Hansen *et al*, 2005).

Analysis of isolated phagosomes showed that the majority of phagosomes contained MHC-I as open conformers with barely any closed conformer present (Fig 5A). Comparing the cells with (dox) or without (no dox) Rab39a, we observed a Rab39a-dependent increase of 25–30% in the number of phagosomes containing open MHC-I in phagosomes as well as an increase in the amount of these Class I conformers per phagosome (~30% increase in MFI) (Fig 5B). In contrast to the increase in open MHC-I in the phagosomes, surface levels of both open and closed MHC-I were unchanged by expression of Rab39a (Fig 5C).

The 64-3-7 antibody used in our assays detected open forms of MHC-I whether or not they are bound to β2-microglobulin (β2m) (Lie *et al*, 1991). It has been shown that β2m-free MHC-I heavy

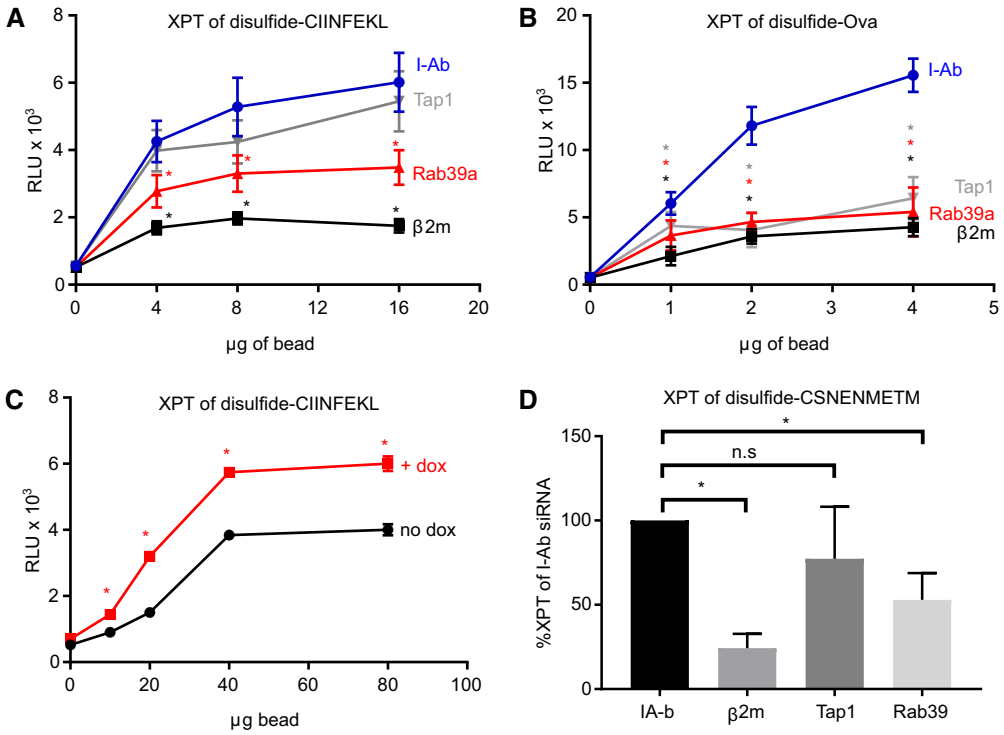

Figure 4. Silencing Rab39a affects the ability of phagosomes to generate peptide–Class I complexes.

A, B XPT of siRNA-treated DC3.2R cells after 48 h of knockdown. Treated cells were fed with the indicated amounts of C8L peptide (A) or Ova (B) conjugated to iron oxide beads via a disulfide bond. The cells were then exposed to RF33.70-Luc Reporter CD8 T cells overnight. Error bars show SD of ≥ 3 replicate wells. *$P \leq 0.05$ for siRNA versus control I-Ab using two-way ANOVA. Representative plot of three independent experiments is presented.

C DC3.2-Rab39a cells (Rab39a KO with dox-inducible Rab39a) were incubated overnight with or without 1 µg/ml dox to induce Rab39a expression. About 1×10^5 cells were then fed with C8L peptide beads and exposed to reporter T cells as in (A). Error bars show SD of duplicate wells. *$P \leq 0.05$ between no dox and + dox using two-way ANOVA. Representative plot of three independent experiments is presented.

D Same as in (A) but cells were fed with 8 µg of A9M peptide bead and exposed to 12.64-Luc Reporter T cells. Experiments were combined by normalizing RLU values to the average of the negative control I-Ab. Error bars show SD of three independent experiments. *$P \leq 0.05$ for Rab39a or β2m siRNA versus negative control I-Ab using ANOVA.

chains can be detected on the surface (Rock *et al*, 1991) and can be utilized in other cell processes besides XPT, such as in NK cell recognition (Arosa *et al*, 2007). Furthermore, open MHC Class I molecule has been shown to be unstable and is internalized for degradation (Ljunggren *et al*, 1990; Mahmutefendic *et al*, 2007). Thus, it was important to determine whether the open H2-L^d enrichment found in the phagosomes of Rab39a-positive cells was actually functional for antigen presentation. To investigate this issue, phagosomes were obtained from null or Rab39a-reconstituted cells, permeabilized *in vitro* with saponin, and pulsed with SPSYVYHQF, a peptide that can bind to H2-L^d (Rice *et al*, 2002). Figure 5D–F show that with peptide, the open H2-L^d in phagosomes decreased, and there was an increase in closed H2-L^d (albeit smaller in magnitude, presumably because the binding of anti-closed conformer antibodies can be affected by the specific peptide that is bound). This showed that at least a fraction of the open conformers in the phagosomes are peptide-receptive and therefore almost certainly β2M-associated heterodimers.

We next examined the effect of BFA on the levels of open MHC-I conformers in phagosomes. To do this, we again isolated and analyzed phagosomes from Rab39a null and reconstituted DC3.2 incubated with BFA and beads. BFA reduced the Rab39a-induced increase in intraphagosomal open conformers (Fig 5G). This finding suggests that Rab39a is increasing the trafficking of open MHC-I conformers and/or affecting phagosomes in ways that stabilize these molecules.

Finally, we wanted to see if the Rab39a-dependent increase in phagosomal open MHC-I molecules was not just limited to H2-L^d but also applied to another MHC-I. Unfortunately, there are no antibodies for other MHC-I molecules that are specific for open conformers like 64-3-7 is for H2-L^d. Therefore, we took the approach of Hansen where we mutated the H2-K^b hinge region (R48Q, R50P) to match that of H2-L^d, thus making it recognizable by the antibody 64-3-7 (Yu *et al*, 1999). As shown in Appendix Fig S2A, open H2-K^b can be detected by 64-3-7, and upon pulsing with SIINFEKL, when these molecules are loaded with S8L peptide, 64-3-7 staining of open conformers is lost and there is an increase in peptide-loaded H2-K^b complexes as assayed by 25-D1 staining. We transduced this construct into our Rab39a-inducible cells and analyzed the levels of open 64-3-7 mAb reactive in phagosomes. Figure EV4A and B shows that just like for H2-L^d, the open form of H2-K^b is also enriched in phagosomes when Rab39a is present. Similarly, the open form of H2-K^b found in the phagosomes are peptide-receptive (Fig EV4C and D). These data are consistent with our findings that

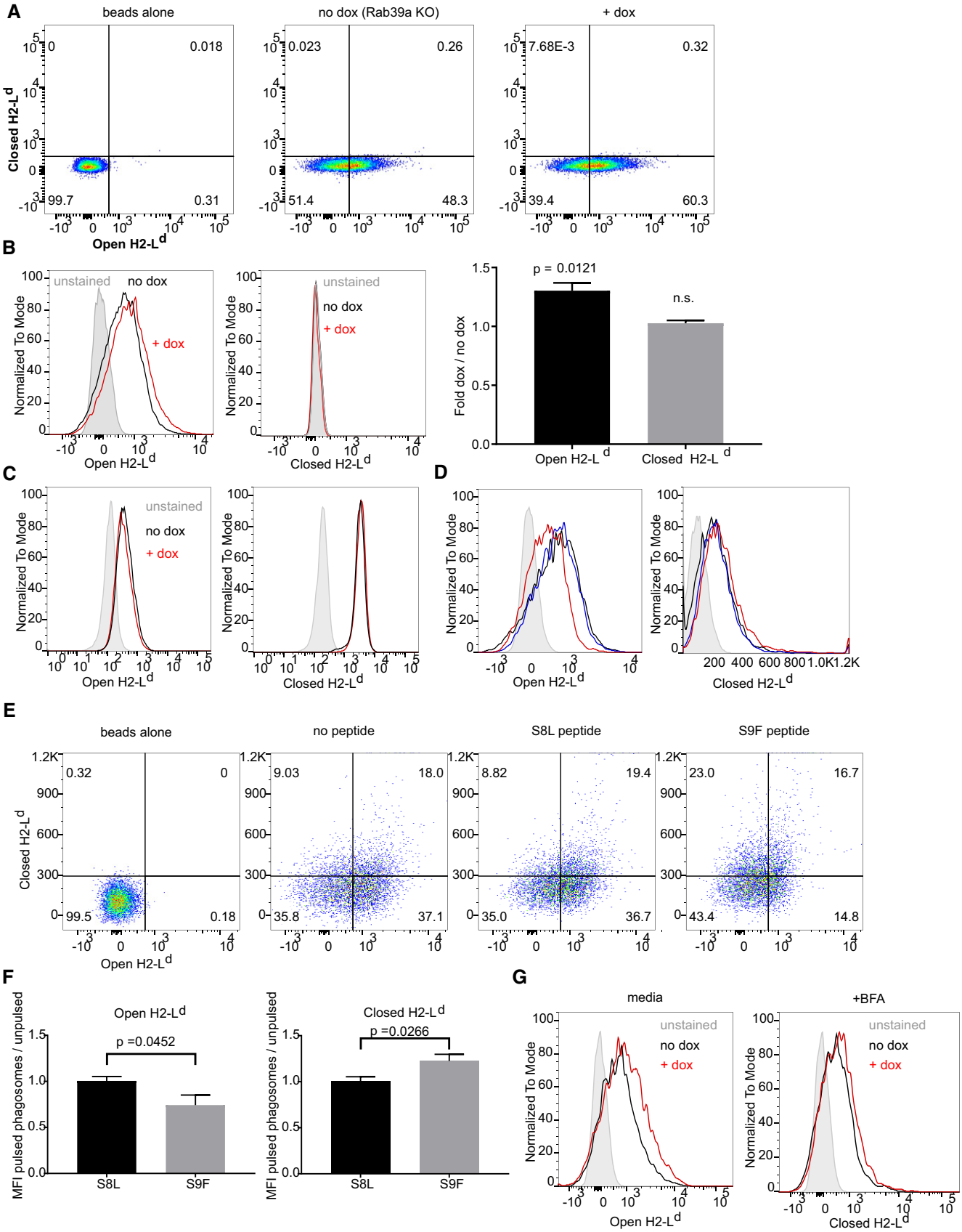

Figure 5.

Figure 5. Effect of Rab39a on intraphagosomal MHC-I molecules.

A, B DC3.2-Rab39a-H2-L^d cells (Rab39a KO with dox-inducible Rab39a) were incubated with or without 1 μg/ml dox overnight to induce Rab39a expression. About 1×10^6 cells were fed at 4 beads/cell of biotinylated magnetic beads for 4 h. Magnetic bead phagosomes were isolated using the listed protocol. Phagosomes were washed, fixed, permeabilized, and stained for open (64-3-7) and closed (30-5-7s) forms of H2-L^d. Representative histograms are shown in (B). The background fluorescence of unstained beads was subtracted from the resulting phagosome gMFI and the fold change of open or closed H2-L^d (dox/no dox) was calculated. Three independent experiments were combined for analysis and error bars show the SD between experiments. Open H2-L^d, but not closed H2-L^d, was statistically significant ($P < 0.05$) between KO and rescued cells using two-tailed ratio-paired Student's *t*-test.

C H2-L^d cell surface levels of KO and induced cells as in (A).

D Phagosomes from KO and induced cells were isolated as in (A). Permeabilized, unfixed phagosomes were incubated with 10 μM of the indicated peptides for 3 h at 25°C in Perm buffer. Phagosomes were then washed and stained for H2-L^d. Shown are histograms of indicated stains.

E Flow cytometry plots of (D).

F Analysis of phagosomes shown in (D) and (E). The background fluorescence of unstained beads was subtracted from the resulting phagosome gMFI and the fold change of pulsed/unpulsed phagosomes was calculated. Shown are *P*-values as computed by two-tailed ratio-paired *t*-test of three independent experiments. Error bars show SD between experiments.

G DC3.2 Rab39a-H2-L^d cells were incubated with or without 1 μg/ml dox overnight to induce Rab39a expression. About 1×10^6 cells were fed at 4 beads/cell of biotinylated-Ova magnetic beads for 4 h in the presence or absence of BFA. Isolated phagosomes were stained for H2-L^d. The result is representative of two independent experiments.

Rab39a promotes MHC-I loading of intraphagosomally targeted minimal peptides for H-2K^b and H2-D^b, which together suggest that Rab39a is affecting this process for all 3 of the major MHC-I molecules (H-2K, H-2D, and H2- L).

Effect of Rab39a on intraphagosomal protein degradation

Open MHC-I molecules are unstable and are likely susceptible to proteolysis in late endosomes/lysosomes (Ljunggren *et al*, 1990). To investigate whether MHC-I conformers were being degraded in phagosomes, we incubated DC3.2-Rab39a-H2-L^d cells in leupeptin (a serine/cysteine protease inhibitor) or bafilomycin (a vacuolar ATPase inhibitor) before extraction of phagosomes. We found that if endosomal proteases were inhibited (Fig EV5A), the number of phagosomes with open MHC-I molecules and the number of these open conformers per phagosome were substantially increased (Fig 6A). Interestingly, the closed form of H2-L^d was not increased after treatment with leupeptin, which is perhaps not surprising because we detect few of these complexes in the phagosomes to begin with and such complexes are more protease resistant. Treatment of cells with bafilomycin was even more effective in increasing the levels and numbers of phagosomes containing open H2-L^d molecules. Interestingly, after the treatment with bafilomycin, we for the first-time detected phagosomes that were "double-positive" for both open and closed forms of H2-L^d. It is possible that this is because bafilomycin not only inactivates proteases due to increasing pH, but can also prevent receptor recycling (Johnson *et al*, 1993). In any case, these data indicate that many open MHC-I conformers are lost in phagosomes due to proteolysis and possibly also due to the effects of low pH. Because of this finding, we sought to determine if Rab39a affected proteolysis in phagosomes, as a reduction in this process might in turn increase the levels of open MHC-I. This could also promote XPT because it has been previously suggested by us and others that hydrolysis of internalized antigen in antigen-presenting cells reduces XPT (Kovacsovics-Bankowski & Rock, 1995; Savina *et al*, 2006).

To analyze this issue, we incubated null or Rab39a reconstituted DC3.2-Rab39a with Ova-conjugated magnetic beads. The resulting phagosomes were then permeabilized and stained with a monoclonal anti-Ova antibody to quantify the amount of Ova, which decreased upon proteolysis. As shown in Fig 6B and C, expression of Rab39a increased the amount of Ova remaining in the phagosome. Interestingly, phagosomes that had the most Ova remaining also enriched the open form of H2-L^d (Fig 6B).

It was conceivable that Rab39a might reduce antigen degradation in phagosomes by reducing fusion with lysosomes. To evaluate this, we looked at the acquisition by phagosomes of the lysosomal membrane protein Lamp1. We found that kinetics of acquisition and level of Lamp1 were unaffected by Rab39a expression (Fig EV5B). This finding was in line with similar observations by other groups in macrophages (Seto *et al*, 2013). Thus, Rab39a was inhibiting antigen degradation in the phagosomes through mechanisms other than interfering with lysosomal fusion.

It has been previously reported the NOX2 complex reduced proteolysis in phagosomes of dendritic cells and that this promoted XPT (Savina *et al*, 2006). NOX2 causes this effect by producing reactive oxygen species (ROS) that alkalinize the vacuoles, which then reduces the activity of acid optimal proteases. Therefore, we investigated whether Rab39a influenced the levels of NOX2 on phagosomes. Phagosomes were isolated from Rab39a null and reconstituted cells and analyzed for their levels of NOX2 by flow cytometry. This analysis revealed that Rab39a increased the levels of phagosomal NOX2 (Fig 6D). To determine if Rab39a expression affected phagosomal ROS, we incubated our knockout and rescued cells with magnetic beads in the presence of CellROX, an ROS indicator dye that fluoresces upon oxidation. This cell permeable dye easily passes through cell membranes, but becomes membrane impermeable upon oxidation, retaining it within intact phagosomes. As shown in Fig 6E, isolated phagosomes from Rab39a reconstituted cells have higher CellROX fluorescence—indicating that these phagosomes had higher levels of ROS as compared to those from Rab39a knockout cells.

Phagosomal proteolysis has also been reported to be reduced through the action of Sec22b. Sec22b is an ERGIC-localized SNARE that was shown to be important in XPT (Cebrian *et al*, 2011; Alloatti *et al*, 2017), although there is conflicting data on this point (Wu *et al*, 2017). Sec22b has been reported to deliver to phagosomes components of the Class I pathway (TAP, tapasin, and calnexin) and enhance phagosome to cytosol transfer of antigens. Moreover, it has been reported to reduce proteolysis in phagosomes. Sec22b has also been shown to allow phagosomal ROS accumulation (Abuaita *et al*, 2015). Therefore, we examined whether Rab39a

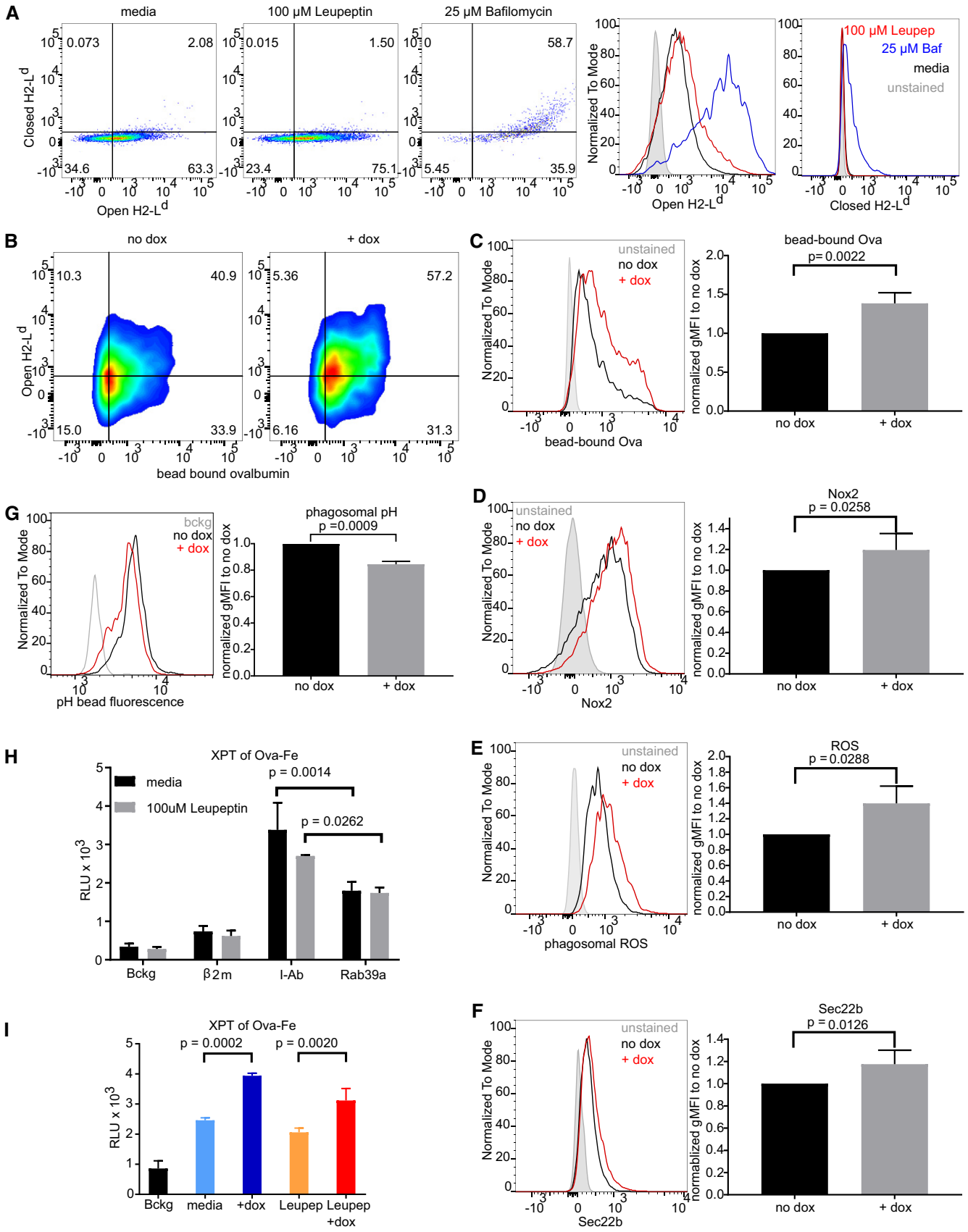

Figure 6.

Figure 6. Effect of Rab39a on intraphagosomal protein degradation.

A DC3.2-Rab39a-H2-L^d cells (Rab39a KO with dox-inducible Rab39a) were incubated with 1 μg/ml dox overnight to induce Rab39a expression. About 1 × 10^6 cells were fed at 4 beads/cell of biotinylated-Ova-magnetic beads for 4 h with the indicated inhibitors. Magnetic bead phagosomes were isolated using the listed protocol. Phagosomes were washed, fixed, permeabilized and stained for Open and Closed (30-5-7s) forms of H2-L^d. Representative histograms of two independent experiments shown.

B Cells as in (A) were incubated with or without 1 μg/ml dox overnight to induce Rab39a expression. About 1 × 10^6 cells were fed at 4 beads/cell of biotinylated-Ova-magnetic beads for 4 h. Phagosomes were isolated and stained for Ova and Open H2-L^d. Representative of three independent experiments.

C, D Quantification of Ova remaining in bead phagosomes (C) and Nox2 staining (D). Representative histogram is shown. For analysis, the background fluorescence of unstained beads was subtracted from the resulting phagosome gMFI and the fold change of target protein (dox/no dox) was calculated. Three independent experiments were combined. $P < 0.05$ using two-tailed ratio-paired Student's *t*-test. Error bars show SD between experiments.

E Cells as in (A) were incubated with or without 1 μg/ml dox overnight to induce Rab39a expression. About 1 × 10^6 cells were incubated on ice with 4 beads/cell of biotinylated-Ova-magnetic beads for bead attachment. Cells were then transferred into media at 37°C containing 5 μM CellROX Deep Red. After 4 h of incubation, unfixed phagosomes were extracted and analyzed via flow cytometry for CellROX fluorescence. For analysis, the background fluorescence of unstained beads was subtracted from the resulting phagosome gMFI and the fold change (dox/no dox) was calculated. Three independent experiments were combined. $P < 0.05$ using two-tailed ratio-paired Student's *t*-test. Error bars show SD between experiments.

F Same as in (C) with Sec22b staining. Three independent experiments were combined. $P < 0.05$ using two-tailed ratio-paired Student's *t*-test. Error bars show SD between experiments.

G Cells as in (A) were fed at 1 bead per cell with pHrodo-conjugated beads that increase fluorescence at low pH. After 4 h of incubation, whole cells were harvested and run through flow cytometry to measure fluorescence of eaten beads. For analysis, the background fluorescence of uneaten beads was subtracted from the resulting gMFI and the fold change of dox/no dox was calculated. Three independent experiments were combined. $P < 0.05$ using two-tailed ratio-paired Student's *t*-test. Error bars show SD between experiments. Also shown are histograms of whole cells compared to background fluorescence of pH beads.

H DC3.2R cells were treated with the indicated siRNA. Forty-eight hours after transfection, cells were fed with Ova-Fe (2 μg Ova) with or without 100 μM leupeptin. RF33.70-Luc reporter T cells were added. After overnight incubation, T cell luciferase was measured. Representative plot of two independent experiments. Error bars show SD between 3 replicate wells. *P* values were calculated using 2-way ANOVA.

I About 5 × 10^4 DC3.2-Rab39a-H2-L^d cells were fed with Ova-Fe (1 μg Ova) with or without 1 μg dox and/or 100 μM leupeptin. RF33.70-Luc reporter T cells were added. After overnight incubation, T cell luciferase was measured. Representative plot of two independent experiments is presented. Error bars show SD between 3 replicate wells. *P* values were calculated using 2-way ANOVA.

influenced Sec22b levels on phagosomes. We found that isolated phagosomes from Rab39a reconstituted cells had small increases in the levels of Sec22b as compared to the Rab39a null cells (Fig 6F).

Increased levels of phagosomal Sec22b, Nox2, and ROS could potentially prevent phagosomal proteolysis through pH modulation. ROS has been shown to alkalinize phagosomes to promote XPT (Savina *et al*, 2006). Thus, we examined whether Rab39a influenced phagosomal pH. To do this, we conjugated beads to pHrodo (Thermo Scientific), a dye that increases fluorescence at decreasing pH. Cells fed with these beads increase fluorescence as their bead-containing phagosomes mature, unless acidification is inhibited with the drug bafilomycin (Fig EV5C). We fed Rab39a (KO or induced) cells with these beads and found that Rab39a increases phagosomal pH (Fig 6G).

The reduction in phagosomal degradation of antigen might also be due to Rab39a-mediated differential recruitment of proteases (such as Cathepsins) to the phagosome. To determine if this is the case, we used SILAC mass spectrometry to quantitatively compare cathepsin levels in phagosomes from Rab39a-sufficient or -deficient DCs. As shown in (Fig EV5D), we did not see consistent significant differences in cathepsin levels in phagosomes from Rab39a KO or induced dendritic cells.

If the reduction in phagosomal catabolism was the sole basis for the Rab39a-dependent augmentation of XPT, then blocking vacuolar proteolysis should restore XPT in Rab39a-deficient cells. To test this, we treated Rab39a-silenced DCs with leupeptin and assayed the effect on XPT. Interestingly, leupeptin did not rescue XPT in the Rab-deficient cells (Fig 6H). Similarly, leupeptin did not eliminate the Rab39a-induced increase in XPT observed when Rab39a expression was induced with dox (Fig 6I). In contrast, leupeptin does inhibit degradation of MHC-I molecules (Fig 6A) and Ova in phagosomes (Fig EV5A). Similar experiments were attempted with bafilomycin but this drug was not compatible with the XPT assay (due to toxicity). Therefore, Rab39a appears to be influencing phagosomes in multiple ways (including at least influences on the levels Sec22b, ROS, pH, proteolysis, and peptide-receptive MHC-I levels) that augment XPT.

Rab39a enhances XPT *in vivo*

To analyze the role of Rab39a in primary DCs as well as in immune responses *in vivo*, we obtained Rab39a knockout mice. The Rab39a gene was disrupted in these mice with a LacZ-containing construct such that beta-galactosidase is expressed in the KO cells that would express Rab39a. Therefore, we were able to use the fluorescent β-galactosidase substrate fluorescein-di-beta-D-galactopyranoside (FDG) (Plovins *et al*, 1994; Chappell & Jacob, 2006), to determine which cells in the mouse spleen express Rab39a. As shown in Fig 7A and Appendix Fig S3A, Rab39a expression was highest on CD11c-positive (dendritic) cells. Within the Cd11c-positive subset, CD8α$^+$ dendritic cells expressed the highest levels of Rab39a, while the Cd11b$^+$ Cd11c$^+$ DCs expressed intermediate amounts. Rab39a was also expressed on a fraction of B220-positive cells (B lymphocytes) and at low levels on CD11b-positive cells (macrophages). We did not see significant differences in cell populations between WT and Rab39a KO mice, including in DC subsets (Appendix Fig S3B). Furthermore, MHC Class I levels in the spleen are not affected by the lack of Rab39a (Appendix Fig S3C).

DCs are the key antigen-presenting cells involved in cross-priming CD8 T cell responses *in vivo*. Therefore, it was of interest to evaluate the effect of the loss of Rab39a on the ability of the primary dendritic cells to XPT antigen. To examine this, we purified CD8α$^+$ DCs (via XCR1) (Bachem *et al*, 2012) and CD8α$^-$ DCs (via DCIR2) (Dudziak *et al*, 2007) (Appendix Fig S3D) and assayed their ability to present Ova-Fe (Fig 7B). XPT by the Rab39a-deficient CD8α$^-$ dendritic cells was partially but significantly reduced. In contrast,

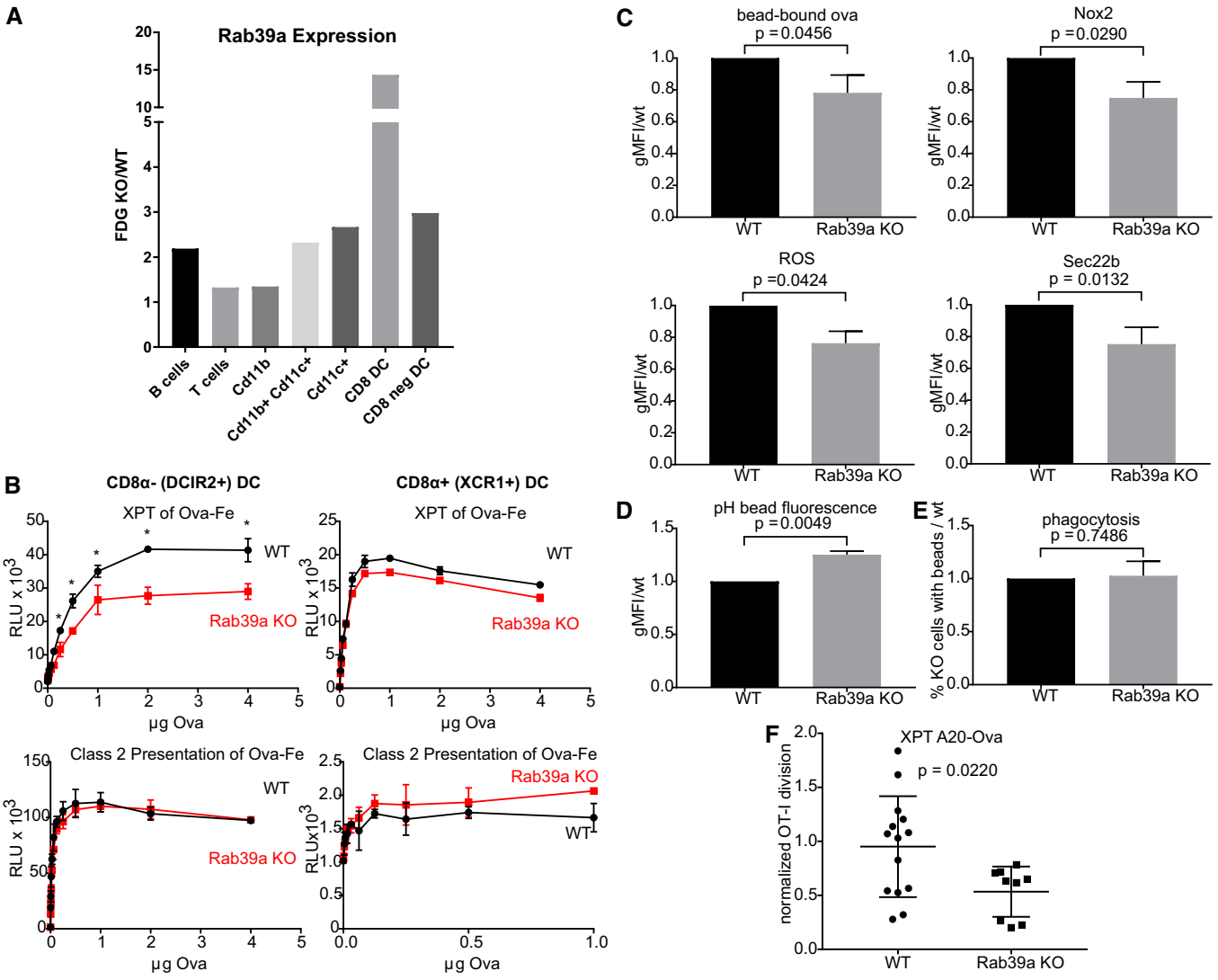

Figure 7. Effect of Rab39a in primary dendritic cells.

A Rab39a expression in splenocyte subsets was measured using an FDG assay. Shown is relative FDG fluorescence of Rab39a KO cells/WT background, which is the summary of two independent experiments.

B Splenic DCs were expanded in Rab39a KO and WT mice by injection of B16-Flt3L tumor. Ten days post-tumor implantation, DCIR2$^+$ (Cd8α$^-$) or XCR1$^+$ (Cd8α$^+$) dendritic cells were isolated from spleens via magnetic positive selection. About 5 × 10^4 cells were plated in a 96-well plate and incubated with the indicated amounts of Ova-Fe and 1:1 of Reporter CD8 or CD4 T cells overnight before measuring luciferase activity. Error bars indicate SD of 2 replicate wells. Shown are representative graphs of three independent experiments. *$P \leq 0.05$ using two-way ANOVA.

C CD11b$^+$ CD11c$^+$ dendritic cells were enriched from WT or Rab39a KO spleens via magnetic negative selection. Cells were fed with 3-µm biotin-Ova-magnetic beads for 4 h. Phagosomes were extracted, permeabilized, and stained for the indicated proteins. For ROS measurements, phagocytosis was performed with 5 µM CellROX and the phagosomes were not permeabilized. For analysis, the background fluorescence of unstained beads was subtracted from the resulting phagosome gMFI and the fold change of target (dox/no dox) was calculated. Shown are three independent experiments combined. Error bars show SD between experiments. *P* values were calculated using two-tailed ratio-paired Student's *t*-test.

D CD11b$^+$ CD11c$^+$ dendritic cells were enriched from WT or Rab39a KO spleens via magnetic negative selection. Cells were fed with 3-µm magnetic beads conjugated to pHrodo. After 4 h, cells were harvested for flow cytometry to measure fluorescence of eaten beads due to phagosomal pH. For analysis, the background fluorescence of uneaten beads was subtracted from the resulting gMFI and the fold change (dox/no dox) was calculated. Shown are three independent experiments with error bars indicating the SD. *P* values were calculated using two-tailed ratio-paired Student's *t*-test.

E CD11b$^+$ CD11c$^+$ dendritic cells were enriched from WT or Rab39a KO spleens via magnetic negative selection. Cells were fed with 3-µm magnetic beads conjugated to Alexa-Fluor dye. After 4 h, cells were harvested and resuspended in 1 mg/ml trypan blue to quench fluorescence of uneaten beads. Cells were run for flow cytometry to measure phagocytosis. The ratio of KO cells with beads/WT cells with beads was then obtained. Graphs show three independent experiments and *P* values were calculated using two-tailed ratio-paired Student's *t*-test. Error bars show SD between experiments.

F Rab39a KO and WT mice were injected intravenously with 1 × 10^5 A20-Ova cells. The next day, CFSE-labeled OT-I splenocytes were injected intravenously. Three days post-OT-I transfer, spleens were harvested, and assayed for OT-I proliferation. Three independent experiments (WT versus KO) were performed. To combine the data, the OT-I proliferation in each individual mouse was normalized to the average proliferation of the WT controls in that experiment. Error bars show SD between individual mice and *P*-value was derived from two-tailed student's *t*-test. *n* = 14 (WT) or 9 (KO).

these same DCs had no defect in MHC-II presentation of the exogenous antigen. The absence of Rab39a, however, did not significantly reduce XPT by CD8α$^+$ DCs. These results showed that Rab39a contributes to XPT *in vitro* primarily in the CD8α$^-$/DCIR2$^+$ dendritic cells.

We then determined if the mechanism of Rab39a in XPT we observed *in vitro* also applied to primary mouse dendritic cells. Isolated CD11b$^+$ CD11c$^+$ dendritic cells (which showed a phenotype in XPT) were fed with magnetic beads, their phagosomes were then isolated, and analyzed via flow cytometry. We found that phagosomal proteolysis, ROS, and the delivery of Nox2 as well as Sec22b to the phagosomes were reduced in Rab39a KO dendritic cells (Fig 7C). Rab39a KO DCs also had more acidic phagosomes as compared to control (Fig 7D). This is despite there being no difference in their ability to phagocytose beads (Fig 7E). Thus, these data replicate our findings in dendritic cell lines and extend them to normal cells.

To evaluate the contribution of Rab39a to XPT *in vivo*, we challenged WT or Rab39a KO mice with cell-associated Ova and then adoptively transferred CFSE-labeled OT-I CD8$^+$ T cells (transgenic T cells specific to SIINFEKL presented on H2-K^b) (Fig 7F). In this experimental setup, the T cells are wild-type while the antigen-presenting cells lack Rab39a. The proliferation of the transgenic T cells was partially but significantly ($P < 0.05$) reduced. These results demonstrated that Rab39a contributes to XPT *in vivo*.

Discussion

The major finding of this report is the identification of Rab39a as a novel component in XPT both *in vitro* and *in vivo*. In contrast, Rab39a did not affect either the presentation of endogenous antigens via the Classical MHC-I pathway or of exogenous antigens on MHC-II molecules. This Rab protein was highly expressed in antigen-presenting cells, particularly in various DC subsets. In DCs, Rab39a trafficking to phagosomes requires transport from the ER/Golgi. Rab39a increased levels of MHC-I molecules in phagosomes and this also required trafficking from the ER/Golgi. Remarkably, these Rab39a-dependent MHC-I molecules were in a peptide-empty conformation and could be loaded with peptides. Rab39a also modified phagosomes by increasing levels of Sec22b, NOX2, and NOX2's reaction products (ROS). This led to increased phagosomal pH and reduced degradation of both antigen and peptide-empty MHC-I molecules. The net effect of the Rab39a-dependent changes was to turn phagosomes into peptide-loading compartments and enhance cross-presentation.

Rab proteins are a large family of small GTPases that control the formation, content, trafficking, and fusion of vesicles in cells (Stenmark, 2009). Our results indicate that Rab39a is functioning in this manner to help deliver vesicular cargo that alters the molecular composition and function of phagosomes in DCs. Previous studies of Rab39a indicated that this Rab protein probably subserves additional functions beyond antigen presentation, as it was also expressed in nonprofessional APCs and affected processes such as neurite morphology (Mori *et al*, 2013), LPS-induced autophagy (Seto *et al*, 2013), and delivery of sphingolipids (Gambarte Tudela *et al*, 2015). Our analysis of Rab39a's effects provides insights into phagosomal regulation and maturation and into the mechanisms of XPT, as discussed below.

There is more than one pathway through which antigens can be cross-presented (van Endert, 2016; Cruz *et al*, 2017). Our studies focused on the P2C pathway because it is the more dominant one *in vivo* for cell-associated antigens and viral infections (Sigal *et al*, 1999; Shen *et al*, 2004). In the P2C pathway, antigens are translocated from phagosomes into the cytosol where they are hydrolyzed by proteasomes into oligopeptides (Kovacsovics-Bankowski & Rock, 1995). These peptides are then usually transported by TAP to MHC-I molecules (Neefjes *et al*, 1993; Kovacsovics-Bankowski & Rock, 1995; Huang *et al*, 1996). Since TAP is an ER-resident protein, it was originally assumed that MHC-I molecules were binding cross-presented peptides in the ER. However, the findings that active TAP was also present on phagosomes raised the possibility of a P2C2P pathway wherein MHC-I peptide-loading occurred within the phagosome (Ackerman *et al*, 2003; Houde *et al*, 2003). Currently, the strongest evidence for this mechanism is that the loss of insulin-regulated aminopeptidase (IRAP), an endosomal aminopeptidase related to ERAP1, reduced XPT (Saveanu *et al*, 2009; Weimershaus *et al*, 2012). This suggested that some cross-presented peptides were trimmed in vesicles, although IRAP may affect phagosomes in other ways (Babdor *et al*, 2017). Our findings that Rab39a augmented XPT and appeared to do so at least in part by promoting intravacuolar peptide-loading provide further independent support for the P2C2P model.

The P2C2P model requires MHC-I molecules to be present in phagosomes and they are indeed found in these vacuoles (Burgdorf *et al*, 2008). However, an unresolved question is how do MHC-I molecules traffic to phagosomes for XPT. A tyrosine in the cytoplasmic tail of MHC-I has been implicated in the delivery of these molecules to phagosomes (Lizee *et al*, 2003). MHC-I molecules are internalized from the plasma membrane (Tse *et al*, 1986; Hochman *et al*, 1991; Basha *et al*, 2008), but it is not clear that these molecules contribute to XPT. MHC-I molecules that are present in an endosomal recycling compartment (ERC) can be delivered to phagosomes via a SNAP23-dependent mechanism (Nair-Gupta *et al*, 2014). However, this may only be involved in XPT during microbial infections because this pathway has been shown to be TLR-dependent (Nair-Gupta *et al*, 2014). In theory, MHC-I molecules could be transported to phagosomes directly from the ER, but up until now evidence of this has been largely lacking. There have been reports that CD74 (invariant chain), which helps traffic MHC-II to endocytic compartments, could also traffic MHC-I to these vesicles (Sugita & Brenner, 1995; Vigna *et al*, 1996; Basha *et al*, 2012). However, in our hands, knock out of CD74 had no effect on P2C cross-presentation either *in vitro* or *in vivo* (Shen *et al*, 2004). Our studies show that Rab39a increased levels of MHC-I molecules in phagosomes. Since BFA blocked delivery of Rab39a and MHC-I molecules, our findings suggest that Rab39a was helping to deliver MHC-I molecules from the ER-Golgi, although it is formally possible that Rab39a was increasing MHC-I molecules in phagosomes via a different mechanism.

Another related and unresolved issue is whether MHC-I molecules are loaded with peptides in phagosomes and if so how this would occur. Our data suggested that at least one of the ways that Rab39a accomplished this was by helping to deliver and/or stabilize peptide-empty MHC-I in phagosomes. Empty MHC-I molecules are readily loaded with peptide and we showed this was the case for the

empty conformers of H2-L^d and H-$2K^b$ (R48Q, R50P). Since peptide-empty MHC-I molecules are unstable, our findings raise, but do not answer, the question as to how these open conformers can be transported to and be present in phagosomes without falling apart. In the ER, these peptide-empty MHC-I molecules are stabilized by chaperones, such as calreticulin (Wearsch & Cresswell, 2008). Since these chaperones have also been reported to be in phagosomes (Ackerman *et al*, 2003; Houde *et al*, 2003), perhaps they are associated with MHC-I molecules during transport. It is possible that Rab39a also created an environment that promoted peptide-loaded MHC-I molecules to exchange peptides. However, for H2-L^d, we detected few peptide-loaded complexes in phagosomes that could be used as substrates for an exchange mechanism.

Interestingly, most phagosomes that had H2-L^d molecules almost exclusively contained these complexes as open conformers. The only situation where we observed phagosomes with both open and closed conformers was when we treated cells with bafilomycin. This same effect was not seen with other agents that inhibited proteolysis (leupeptin) and therefore the absence of closed conformers was unlikely to be due to their degradation. Bafilomycin can interfere with the recycling of molecules (Johnson *et al*, 1993; Baravalle *et al*, 2005) and perhaps this was why this agent caused the accumulation of closed MHC-I conformers in phagosomes. Previous reports have described that peptide-loaded MHC-I complexes were rapidly recycled (Mahmutefendic *et al*, 2011, 2013). Therefore, in the absence of bafilomycin, the MHC-I molecules that were loaded with peptides in the phagosome may have been rapidly exported, perhaps in a manner similar to what occurs when these molecules bind peptides in the ER.

We found that Rab39a increased phagosomal levels of NOX2 and ROS, increased pH value, and reduced protein degradation. This is consistent with previous reports that NOX2 was recruited to phagosomes and reduced protein hydrolysis through ROS generation leading to alkalization of the vacuole (Savina *et al*, 2006) and provides insight into the mechanism of this recruitment. Preventing vacuolar acidification has been reported by us and others to enhance XPT and up until now the underlying basis for this effect was suggested to be reduced antigen destruction. However, our findings suggest an additional underlying mechanism as well. We found that the open conformers of H2-L^d were very susceptible to degradation in phagosomes. In DCs, the highest levels of open conformers were found in the phagosomes that were least hydrolytic and in other phagosomes the levels of these conformers could be markedly increased by inhibiting proteolysis. Therefore, the Rab39a-NOX2-dependent reduction in proteolysis may be needed to preserve antigen as well as peptide-receptive MHC-I molecules for XPT. In addition, however, Rab39a must be contributing to XPT in ways other than just reducing proteolysis, because protease inhibitors, which increased levels of open conformers, did not restore XPT in Rab39a-silenced cells.

We found that Rab39a increased levels of Sec22b on phagosomes. Sec22b is a SNARE protein that allows transport vesicles to fuse with their target vesicles (Cebrian *et al*, 2011; Alloatti *et al*, 2017). Sec22b had previously been implicated in the delivery of components from the ER to phagosomes and promoting XPT (Cebrian *et al*, 2011). What targeted Sec22b containing vesicles to phagosomes was unknown. Our results suggest that Rab39a is one of the targeting mechanisms. The role of Sec22b in XPT was recently questioned (Wu *et al*, 2017); however, our findings are consistent with the original conclusions that this SNARE protein contributes to XPT. Thus, Rab39a appears to help deliver several components that are needed for optimal XPT, including, e.g., NOX2, MHC-I, and likely Sec22b-delivered cargo, such as TAP (Cebrian *et al*, 2011).

Our data add to an evolving picture of phagosomal maturation in which there is no single program of maturation but rather that this is a complex and multifaceted process that can lead to different fates. Rab39a does not affect phagosomal acquisition of lamp1 or of Rab7, both markers of "classical phagosome maturation". Thus Rab39a-dependent acquisition of ER components is apparently independent of classical phagosome maturation. Moreover, the end point of classical maturation is to create a highly catabolic vacuole and Rab39a opposes this fate. Similarly, the delivery of the components needed for MHC-II presentation to phagosomes is independent of Rab39a. It will be of interest in future studies to investigate whether these various events produce distinct subsets of phagosomes that subserve different functions in the same cell versus affecting the fate of all phagosomes in a cell in the same manner.

Interestingly, the wild-type form of Rab39a, but not GDP-locked and GTP-locked Rab39a mutants, could enhance XPT of bead-bound antigen. These data suggest that the proper cycling of Rab39a from the GDP to the GTP-bound form (and back) was important for XPT. A similar requirement of cycling through GDP- and GTP-bound forms has been described for Rab22a, which is involved in recycling of cell surface molecules including MHC Class I (Weigert *et al*, 2004), as well as some other Rab proteins (van Weering *et al*, 2007; Fukuda *et al*, 2008).

We documented a contribution of Rab39a to XPT in multiple different professional APCs, but interestingly the extent of this contribution varied. There was a relatively large contribution in myeloid-derived DC clones. Among primary DCs, loss of Rab39a reduced XPT the most in $CD8\alpha^-$ dendritic cells ($DCIR2^+$). This dendritic cell subset is known to cross-present antigen *in vivo* (Dudziak *et al*, 2007). In contrast, the loss of Rab39a in primary $CD8\alpha^+$ dendritic cells ($XCR1^+$), which are the most active cross-presenting subset in many situations (Bachem *et al*, 2012), resulted in an insignificant reduction in cross-presentation. The differences in the magnitude of the Rab39a effects in different antigen-presenting cells might arise from differences in the levels of redundant mechanisms, adaptations to the loss of Rab39a, and/or the relative activity of P2C-to-ER versus P2C2P pathways. Interestingly, compared to $CD8\alpha^+$ dendritic cells, the $CD8\alpha^-$ subset is much more active in presenting antigens on MHC-II (Dudziak *et al*, 2007), and perhaps this is one of the reasons that the latter subset is more dependent on Rab39a (e.g., to reduce the hydrolytic activity in phagosomes). In any case, the net effect of losing Rab39a is a reduction of cross-priming *in vivo*.

Materials and Methods

Mice

All mice were maintained at University of Massachusetts Medical School in a specific pathogen-free facility, and all mouse experiments were carried out under an approved IACUC protocol.

Rab39a knockout mice were generated by the Knockout Mouse Project (KOMP). OT-I mice express a transgenic T cell receptor

against SIINFEKL on H2-K^b (Hogquist *et al*, 1994). OT-I mice were bred with CD45.1 mice for a congenic marker. Control mice were C57BL/6NJ. All mice were originally obtained from the Jackson Laboratory. Mice were gender- and age-matched (≥ 6 weeks of age) for each experiment.

Cell culture media

Cells were maintained in hybridoma culture media (HCM) composed of RPMI 1640, 10% FCS, 1× HEPES, 1× nonessential amino acids, 1× antibiotic-antimycotic, 1× L-glutamine, and 54 μM 2-mercaptoethanol. Experiments that needed media lacking reducing agents used complete DMEM (cDMEM) (which lacks glutathione) that was supplemented with all the HCM supplements except 2-mercaptoethanol.

Antibodies

The following antibodies against the listed proteins were used: H2-K^b (Af6-88.5, BD), I-A/I-E (M5/114.15.2, BD), CD107a (1d4B, BD), CD107b (ABL-93, BD), Ova (Ova-14, Sigma), HA-tag (6E2, Cell Signaling), HA-tag (C29F4, Cell Signaling), H2-L^d closed conformer (30-5-7s, Thermo), H2-L^d open conformer (64-3-7, Dr. Clifford Harding, Case Western Reserve University), Sec22b (Rabbit, Synaptic Systems), b-actin (C4, Santa Cruz), CD45.1 (A20, Thermo), CD8a (53-6.7, Thermo), CD45R (RA3-6B2), CD11b (M1/70, Thermo), CD11c (N418, Thermo), XCR1 (REA707, Miltenyi), DCIR2 (33D1, Biolegend), CD3e (145-2C11, Thermo), Nox2 (Clone 53, BD), TCRb (H57-597, BD), Fc block (2.4G2, ATCC), SIINFEKL-H2-K^b (25-D1, Thermo), CD19 (1D3, BD), Thy1.2 (53-2.1, BD), CD36 (HM36, Biolegend), F4/80 (BM8, Biolegend), and Ly6-C/G (RB6-8C5, BD). Secondary antibodies (goat anti-mouse IgG2a, IgG2b, IgG1, IgG and donkey anti-rabbit IgG) were purchased from ThermoFisher. HRP-conjugated secondary antibodies were purchased from Jackson Immunoresearch.

Dendritic and macrophage cell lines

DC2.4 and DC3.2 are J2 virus-immortalized dendritic cell clones (Shen *et al*, 1997). IMMP are J2 virus immortalized bone marrow-derived macrophages (Hornung *et al*, 2008).

DC3.2R is a clone of the DC3.2 cell line transduced with a lentiviral construct expressing Renilla luciferase. This construct was made by amplifying the thymidine kinase–Renilla luciferase insert from plasmid pRL-Tk (Promega) and inserting it into the lentiviral vector pCDH1-CMV-MCS-EF1-Puro. Renilla luciferase expression was originally used as a viability marker in screening experiments. DC3.2R was chosen for the present study because it coincidentally had very good XPT and MHC-II presentation abilities as compared to other DC clones.

DC3.2 NS-Ova is a variant of DC3.2 that expresses a nonsecreted form of ovalbumin (Ova) upon induction with doxycycline (dox). To construct this cell, the gene for chicken Ova (Shen & Rock, 2004) was amplified without the first 50 amino acids encoding the secretion signal, replacing it with a methionine. The insert was put into the Age-I Mlu-I sites of pTRIPZ (Open Biosystems) for lentiviral production and transduction of DC3.2. pTRIPZ contains the tet-on promoter system allowing dox-inducible expression of cloned genes.

DC3.2 UbS8L was transduced with Ubiquitin-S8L (York *et al*, 2006; Towne *et al*, 2007) in the pTRIPZ lentiviral vector and in the presence of doxycycline expresses the SIINFEKL peptide fused to the C-terminus of ubiquitin.

Luciferase expressing T cell hybridomas

The RF33.70 cell line is a CD8$^+$ T cell hybridoma that recognizes the Ova peptide SIINFEKL on H2-K^b (Rock *et al*, 1990a). MF2.2D9 is a CD4$^+$ T cell hybridoma that recognizes Ova$_{258–276}$ on I-A^b (Rock *et al*, 1993). 12.64 is a CD8$^+$ T cell hybridoma recognizing the ASNENMETM peptide of the influenza peptide NP366 (Deckhut *et al*, 1993). These three T cell hybridomas were transduced with lentivirus containing NFAT-Luciferase which was constructed by cloning the NFAT-Luciferase insert from plasmid pGL3-NFAT luciferase (A gift from Jerry Crabtree, Addgene plasmid #17870) (Clipstone & Crabtree, 1992) into pCDH1-CMV-SV40-Bsd. This backbone vector is a modification of pCDH1-CMV-MCS-EF1-Puro wherein the EF1-Puro region was replaced with the blasticidin resistance gene under the SV40 promoter.

The 12.64-luc cell was previously described (Kincaid *et al*, 2011).

A20-Ova cells

To generate a source of cell-associated antigen for XPT, the Balb/c B cell lymphoma A20 was lentivirally transduced with a membrane-bound Ova construct. The secretion signal of Ova was removed (first 50 amino acids) and the Ova fragment was fused to the N-terminal region of mouse Clec2d. This localized Ova to the cytosolic side of the cell membrane. The Ova-Clec2d construct was cloned into the modified pCDH1-blasticidin vector described above.

Gene manipulation experiments

siRNA transfections

The siRNAs used were SiGenome smartpools purchased from Dharmacon. To transfect dendritic cell lines, the protocol for Lipofectamine RNAiMax (Invitrogen) was used under the following conditions: Each well of a 384-well plate was seeded with a mixture containing 0.2 μl of RNAiMax, 6.8 μl of 1× siRNA buffer (Dharmacon/GE), and 3 μl of 0.5 μM siRNA. The mixture was incubated for 20 mins at room temperature. Then, 20 μl of dendritic cells (total of 2.5×10^3) in RPMI 1640 with 15% FCS were added. The plate was spun down at 200× *g* for 1 min and incubated for 48 h prior to assays. At other times, the procedure was performed in 96-well or larger welled plates, with the conditions scaled up by multiplying cell numbers and reagents to the ratio of well surface areas.

Quantitative PCR

After siRNA treatment of cells, total RNA was extracted using an RNeasy Mini Kit (Qiagen) according to manufacturer instructions. Quantitative PCR was performed using Luna Universal One-Step RT-qPCR kits (New England Biolabs) in a Bio-Rad CFX96 cycler. HPRT was used as housekeeping control and relative expression was calculated using $\Delta\Delta C_T$ method. The primers used were HPRT (5′-AGGGATTTGAATCACGTTTG-3′ and 5′-TTTACTGGCAACATCAACAG-3′) and Rab39a (5′-CGCTTCAGATCAATAACTCG-3′ and 5′-TGTCCCACCAGTAGAAATAC-3′).

Lentiviral transduction of cell lines

Lentivirus was produced by transfecting HEK-293T (ATCC) cells with the viral construct containing the gene of interest along with equimolar amounts of the plasmids Delta8.9 and VSVg (gifts from Dr. Eicke Latz, UMASS Medical School). Transfection conditions were done according to the Lipofectamine 2000 protocol (Invitrogen). Twenty-four hours post-transfection, cell culture media was replaced. The viral supernatant at 48 h was collected and filtered through a 0.45-μm syringe filter. About 1×10^5 target cells were seeded in 6-well plates. The next day, media was removed and replaced with 1:1 mix of viral supernatant and HCM with 5 μg/ml polybrene (Sigma-Aldrich). After 24 h, cell media was replaced. After 48 h post-infection, 5 μg/ml of puromycin or blasticidin (depending on the vector) was added. Cells were maintained in antibiotic media for at least 2 weeks, replacing media with fresh antibiotic every 2 days.

Creation of Rab39a CRISPR knockout and inducible cells (DC3.2-Rab39a)

Rab39a was knocked out at the genomic level using CRISPR/Cas9. The target sequence was elucidated using an algorithm as described (Hsu *et al*, 2013). The guide sequence of gtgatcggagactccacggt was chosen because it had an endogenous restriction site (BtgI) within the CRISPR cutting site. This allowed screening of clones via restriction enzyme digestion. The guide sequence was inserted into CRISPR plasmid pX330-U6-Chimeric_BB-CBh-hSpCas9 (Addgene plasmid #42230) (Cong *et al*, 2013) and a gfp cassette was PCR amplified from pEGFP-N1 (Clontech) and inserted within the Nar1 site of the CRISPR plasmid.

About 2×10^6 DC3.2 cells were electroporated with 2 μg of the CRISPR construct using Amaxa nucleofector II with program T-030 and Cell Line Nucleofector Kit V. Cells were allowed to recover overnight in HCM. GFP expressing cells were flow sorted into 96-well plates at 1 cell per well (UMASS Medical School Flow Cytometry Core Facility).

The sorted DC clones were screened by DNA sequencing. DNA samples from clones were extracted using a DNeasy Blood and Tissue Kit (Qiagen). A region of Rab39a containing the CRISPR target site was PCR amplified using primers 5′-AGGTGCTGAAGG GACAGTTC-3′ and 5′-AAACTGCGGAGGAGGAAGTC-3′. PCR products were screened by cutting with BtgI (New England Biolabs). Successful mutations generated by CRISPR destroyed this restriction enzyme site. PCR products that resisted digestion were cloned into PCR2.1-TOPO (Invitrogen) according to manufacturer instructions. For every dendritic cell clone, 10 bacterial clones were sequenced to check mutations in the CRISPR target site. Clones that showed exactly 2 different mutations (which indicated that both alleles of the gene were disrupted) were chosen.

For Rab39a rescue experiments, a Rab39a CRISPR clone of DC3.2 was transduced with a lentiviral vector containing dox-inducible Rab39a (DC3.2-Rab39a cells). The cDNA for Rab39a was amplified from C57BL/6 cDNA, with an HA-tag added on the N-terminus. This construct was inserted within the Age1–Mlu1 sites of the plasmid pTRIPZ (GE Dharmacon). Lentivirus production and DC transduction were performed as described. Selection was done at 5 μg/ml puromycin. Knockout cells were rescued with Rab39a by adding 1 μg/ml dox (Sigma Aldrich).

Some experiments necessitated that DCs express the MHC-I molecule H2-L^d. A C-terminal myc-tagged H2-L^d was synthesized and inserted into the lentiviral vector pCDH1-CMV-SV40-Bsd. The Rab39a-inducible cells described above were transduced using this lentiviral construct (DC3.2-Rab39a-H2-L^d cells). Other experiments needed that DCs express H2-K^b that is recognized by the antibody 64-3-7. To achieve this, a mutated H2-K^b construct (R48Q, R50P) (Yu *et al*, 1999) was synthesized and transduced to the above cells.

Rab39a KO cells were also rescued with mutant forms of Rab39a. The GDP-locked form generated with a S22N mutation and a GTP-locked form was generated through a Q72L mutation (Seto *et al*, 2011).

Antigen presentation assay

To plated antigen-presenting cells, the listed concentrations of Ova-conjugated beads or soluble Ova were added along with a 1:1 (DC:T cell) number of luciferase expressing reporter T cells. After overnight incubation, luciferase expression by the T cells was measured using Oneglo reagent (Promega) according to manufacturer instructions. The luminometer used was an Envision (Perkin Elmer) equipped with ultra-sensitive luminescence module.

Antigen beads

Biomag-Ova beads (Ova-Fe)

Biomag-Ova beads (Ova-Fe) are magnetic particles (Iron oxide) covalently conjugated to Ova. BioMag Amine and BioMagPlus Amine Protein Coupling Kit were purchased from Bangs Laboratories. Chicken Ova was purchased from Sigma-Aldrich. Protein conjugation was performed using the glutaraldehyde method according to bead manufacturer instructions. Briefly, beads were washed in pyridine buffer and activated with 5% glutaraldehyde for 4 h. The beads were then washed and incubated with 5 mg/ml Ova dissolved in pyridine buffer overnight. Beads were extensively washed and resuspended in PBS. Ova concentration on the beads was measured using absorbance at 280 nm of pre- and post-coupling solutions.

Peptide and disulfide linked beads

Iron oxide beads with antigens conjugated through disulfide bonds were made by first reacting Biomag Amine beads with SPDP (succinimidyl 3-(2-pyridyldithio)propionate) (Thermo Scientific) according to manufacturer instructions. These beads were then incubated overnight at room temperature with cysteine containing peptides (Genscript, in 50% DMSO) or cysteine-modified Ova. After incubation, beads were extensively washed with PBS.

Cysteine-modified Ova was produced by reacting 1 ml of 1 mg/ml Ova with 10 μl of 2 mg/ml Traut's Solution (2-iminothiolane in PBS, Thermo Scientific). The reaction was performed in PBS for 30 min at room temperature.

Latex-Ova beads (Ova-Latex)

Latex-Ova beads are polystyrene beads covalently conjugated to Ova. About 1-μm polystyrene latex (amine group modified) beads were purchased from Bangs Laboratories. Beads were washed with PBS and incubated with 10% glutaraldehyde (Thermo Scientific) for 2 h. Beads were washed twice with PBS and incubated with 5 mg/ml of Ova in PBS overnight. Beads were then washed and resuspended in PBS.

Assaying the Classical Pathway with NS-Ova and UbS8L

The DC3.2 NS-Ova and DC3.2 UbS8L cells were transfected with the indicated siRNA. After 48 h of silencing, dox was added at the listed concentrations. After the indicated period of time, reporter T cells (corresponding to 1:1 ratio with DCs) were added along with a final concentration of 1:1,000 brefeldin A (Golgiplug, BD) to stop further egress of H2-K^b–SIINFEKL to the surface. The cells were incubated overnight, and luciferase expression of the T cells was measured.

Peptide pulsing experiments

Tap1 KO DC3.2 cells were made using CRISPR (Guide: GGCGGCCGCCCTGCTCCTTC). A mutated H2-K^b construct (R48Q, R50P) was transduced to these KO cells. The Tap KO DCs were incubated overnight at 25°C to increase levels of open MHC-I molecules on the surface (Ljunggren *et al*, 1990). The next day, SIINFEKL (S8L, for H2-K^b R48Q, R50P) or SPSYVYHQF (S9F for H-2L^d) peptides at varying concentrations were added. The cells were incubated at 25°C for 2 h before washing and staining for flow cytometry.

Staining and confocal microscopy

Fixed cell microscopy

For fixed cell imaging, cells were grown on coverslips overnight. The next day, cells were washed and fixed with 4% PFA for 10 min. Cells were subsequently permeabilized, stained in 0.25% saponin, 1% BSA in PBS, and mounted in ProLong Antifade (Thermo Scientific). Cells were imaged under a Leica TCS SP5 confocal microscope. Image analysis and processing were done in ImageJ software.

Live cell microscopy

For live cell imaging, Rab39a KO DC3.2 cells were transduced with lentivirus containing inducible Rab39a fused with an N-terminal mcherry construct. Cells were grown to 70% confluency in 7-mm glass bottom dishes (MatTek Corporation) with 1 μg/ml dox overnight. The next day, cells were fed with fluorescently labeled 3-μm polystyrene beads (Bangs Laboratories) for 2 h. Cells were imaged live under a Leica TCS SP5 confocal microscope. Image analysis and processing were done in ImageJ software.

Phagocytosis assay

To assay for phagocytosis, cells were incubated with fluorescently labeled magnetic beads (Amine containing Promag beads, Bangs Laboratories). These beads were made by conjugating their amine groups with Alexa-Fluor NHS reagent (Thermo Scientific). Cells were incubated with beads (5:1 bead-cell ratio) on ice for 30 min to allow binding. The cells were then transferred into 1.5 ml tubes containing prewarmed media and kept at 37°C in a water bath. After 1 h, cells were spun down and resuspended in ice-cold 1% serum-PBS buffer. Just prior to analysis, trypan blue (Thermo Scientific) was added at a final concentration of 1 mg/ml to quench the fluorescence of uneaten beads. The mixture was put on ice for 1 min and then run through a flow cytometer to measure fluorescent cells that had eaten the beads.

Phagosome flow cytometry

To make biotinylated 6-μm magnetic beads, COMPEL COOH (Bangs Laboratories) were conjugated to biotin hydrazide (Covachem) using EDC (Thermo Scientific).

To make biotinylated Ova beads, COMPEL COOH beads were conjugated with ovalbumin (Sigma Aldrich) using EDC. After extensive washing, beads were conjugated to Biotin-NHS (Thermo Scientific) using manufacturer instructions.

DCs were incubated at 37°C with various biotinylated beads (number and time indicated in figure legends) to allow phagocytosis. Cells were then washed with PBS, detached with Versene (Thermo Scientific) for 5 min at 37°C, and then harvested.

To label uneaten or surface-bound beads, cells were first stained with 6.4 μg/ml of Streptavidin Pacific Blue or Orange (Thermo Scientific) in 1% FCS-PBS for 10 min on ice. After washing in 1% FCS-PBS, cells were then resuspended in ice-cold homogenization buffer (HB) containing 250 mM sucrose and 10 mM $CaCl_2$ with 1× HALT EDTA-free protease inhibitor (Thermo Scientific). Cell disruption was performed in a 0.3 ml dounce homogenizer (Kimble Chase) using the tight fitting "B" pestle. The extent of homogenization was observed under a microscope and cells were dounced to at least 50% lysis while minimizing disruption of the nucleus. Phagosomes were then isolated with a magnet. Centrifugation in this and subsequent steps was not used to avoid artefactual fusion of membranes.

To distinguish between intact and ruptured phagosomes, phagosomes were washed in wash buffer (1% BSA in PBS) and stained once again with streptavidin pacific blue/orange for 10 min. After extensive washing with magnetic separation, phagosomes were fixed in 2% paraformaldehyde for 20 min or directly permeabilized and stained.

For staining, the isolated magnetic bead phagosomes were incubated for 10 min in Perm Buffer (1% BSA in PBS with 0.25% saponin). Phagosomes were stained with the indicated antibodies. For FACS analysis, phagosomes were resuspended in wash buffer.

For flow cytometric analysis of intact phagosomes, events were gated according to the FSC and SSC of plain magnetic beads as well as the lack of Pacific Blue/Orange staining (allowing exclusion of uneaten beads and ruptured phagosomes).

Phagosome flow cytometry for primary dendritic cells

Isolated primary dendritic cells were incubated with the indicated beads and phagosomes were extracted according to the above protocol. Unless otherwise stated, beads were 3 μm in size (Promag3, Bangs Laboratories) instead of 6 μm used in the cell lines because the primary dendritic cells had more difficulty that the DC cell lines in ingesting the larger beads.

Peptide loading of phagosomes

Isolated, unfixed phagosomes were permeabilized in ice-cold Perm Buffer supplemented with 1× HALT protease inhibitor (Thermo Scientific). Peptide was added (nature and concentration were dependent on the experiment) and the mixture was rotated at room temperature for 3–4 h. The phagosomes were washed extensively in Perm Buffer before staining for flow cytometric analysis.

Phagosomal ROS assay

About 5×10^5 dendritic cells were incubated with the indicated beads and plated into 24-well plates containing media with 5 μM CellROX Deep Red, an ROS indicator (Thermo Scientific). After the indicated timepoint, cells were detached and phagosomes were isolated. Isolated, unfixed phagosomes were analyzed in a flow cytometer.

Assaying phagosomal pH

Carboxy magnetic beads (Compel-COOH, Bangs Laboratories) of size 6 μm were conjugated to lysine using EDC (Thermo Scientific) in order to add amine groups to the beads. pHrodo Green STP ester (Thermo Scientific) was then conjugated to the beads using the manufacturer's protocol.

Dendritic cells were fed (time and bead number indicated in the experiment) with the pHrodo green beads. Cells were then washed and harvested for flow cytometry to measure fluorescence of the ingested beads. For experiments with bafilomycin, the drug was used at 25 nM and was added to the cells simultaneous with the beads.

Mouse experiments

FDG assay for detection of beta-galactosidase expression

Rab39a knockout mice contain the beta-galactosidase gene under the control of the Rab39a promoter (KOMP). The expression of β-gal was measured using Fluorescein di-β-D-galactopyranoside (FDG). The protocol described below is a modification to previously published work (Plovins *et al*, 1994; Chappell & Jacob, 2006).

Single-cell suspensions of spleens were obtained from WT and Rab39a KO mice. About 20×10^6 cells were resuspended in 200 μl of PBS and warmed to 37°C for 10 min in a water bath. Then an equal amount of prewarmed 4 mM FDG in distilled water (Setareh Biotech) was mixed and added to the cells. After 2 min at 37°C, ice-cold staining buffer (1% FCS in PBS) was added to the cells. The cells were then stained at 4°C with antibodies for flow cytometry.

Ex vivo antigen presentation assay

To generate large amounts of dendritic cells, 5×10^6 B16-FL cells were injected subcutaneously into the nape of mice. B16-FL cells secrete Flt3 ligand which promotes dendritic cell development (Mach *et al*, 2000). Ten to twelve days after injection, the enlarged spleens of mice were harvested.

Spleens were perfused with and soaked in digestion medium (400 U/ml Collagenase Type II, 1 μg/ml DNAse in HBSS with Ca^{2+} and Mg^{2+}) for 30 min at 37°C. The digested spleens were pressed through a 70-μm filter to generate a single-cell suspension. After washing with 1% FCS-PBS, Fc receptors were blocked with 2.4G2 supernatant and cells were stained with biotinylated antibodies. Anti-XCR1 was used to isolate $CD8\alpha^+$ DCs, while 33D1 antibody (against DCIR2) was used to isolate $CD8\alpha^-$ DCs. The stained cells were washed and purified using streptavidin Dynabeads (M-280, Thermo Scientific). Isolated cells were counted and plated for antigen-presentation assays with reporter T cells.

In vivo XPT assay

Spleens from OT-I mice were isolated, red blood cells were lysed, and single-cell suspensions were obtained. Splenocytes were labeled with 1 μM carboxyfluorescein succinimidyl ester (CFSE, Thermo Scientific) for 10 min in PBS at 37°C. Cells were washed and resuspended in 1% FCS in PBS at 10×10^6 cells/ml. About 100 μl of cells was injected into mice intravenously via retro-orbital injection. Antigen was delivered to the mice 1 day prior to injection of OT-I cells.

Three days after OT-I injection, mice were sacrificed and spleens harvested. The harvested cells were stained for CD8α and CD45.1 to measure OT-I proliferation using a flow cytometer.

Isolation of $Cd11b^+$ $Cd11c^+$ splenic dendritic cells for phagosome flow cytometry

$CD11b^+$ $CD11c^+$ "bead-free" dendritic cells were enriched via magnetic negative selection. Mouse spleens were dissociated with Collagenase/DNAse and single-cell suspensions were prepared. After lysis of RBCs, the cells were stained (1 μg in 500 μl of 1% FCS in PBS) with biotinylated antibodies against CD19, Thy1.2, CD36, F4/80, XCR1, CD8α, and Ly-6C/G. Cells were washed and incubated with 5×10^9 150-nm streptavidin beads (Ocean Nanotech) for 20 min. Bead-free cells were harvested using a magnet.

Silac experiments

To perform SILAC, DC3.2-Rab39a cells (Rab39a KO with dox-inducible Rab39a) were grown in light (R0K0) or heavy (R10K8) DMEM with 10% dialyzed FCS (DC Biosciences). The cells were grown in the respective media for 2 weeks to achieve complete isotope incorporation. Cells grown in heavy media were induced with 1 μg/ml doxycycline overnight to induce Rab39a expression. About 4×10^7 each of KO and induced cells were fed with 4 beads per cell of 6-μm biotinylated magnetic beads. After 4 h of phagocytosis, intact phagosomes were obtained using dounce homogenization and streptavidin-fluor staining as listed above. Pure intact phagosomes were separated from debris and unbroken cells via flow sorting. The phagosomes were then washed and lysed in Nupage LDS Sample Buffer with dithiothreitol (Invitrogen). Equal amounts of lysate were mixed (normalized to yield in flow sorting) and run in a short protein gel. The gel was Coomasie Blue stained and the accumulated protein band was cut and sent to the UMASS Medical School Mass Spectrometry Facility for mass spectrometry analysis. Three independent experiments were performed (biological replicates), and within each experiment, samples were analyzed in triplicate (technical replicates).

Analysis was done using Scaffold (Proteome Software).

Quantification and statistical analysis

Unless otherwise stated, data are shown as the mean ± standard deviation (SD). Analysis was done with Graphpad PRISM and the method of analysis is listed in the figure legends. For flow cytometry of isolated phagosomes as well as measurements of phagosomal pH, background fluorescence of uneaten magnetic beads (or pH sensing beads) was first subtracted before analysis and background values are given in the figure legends.

Data availability

The datasets and computer code produced in this study are available in the following databases:

- siRNA Forward Genetic Screen: BioStudies S-BSST306 (https://www.ebi.ac.uk/biostudies/studies/S-BSST306)
- Phagosome proteomics data: MassIVE MSV000084611 (https://massive.ucsd.edu/ProteoSAFe/dataset.jsp?task = deff5e57b0714d7d869810db1d0d0dd2)

Expanded View for this article is available online.

Acknowledgements
We would like to thank the members of the Harvard ICCB-Longwood facility for their help and support in setting up an RNAi screen which led to the elucidation of Rab39a. We thank Dr. Diego J.Farfán-Arribas, Dr. Lianjun Shen, and Dr. Elena Merino-Rodriguez for providing cell lines, constructs, and technical assistance. We thank Dr. Scott Shaffer and Dr. John Leszyk of the UMASS Mass Spectrometry facility for our mass spectrometry experiments. This work was supported by Grant AI114495 from the NIH.

Author contributions
FMC conceived the study, designed and performed the experiments, analyzed and interpreted the data, and wrote the manuscript. KLR conceived and supervised the study, and wrote the manuscript. JDC designed and performed experiments as well as analyzed the data.

Conflict of interest
The authors declare that they have no conflict of interest.

References

Abuaita BH, Burkholder KM, Boles BR, O'Riordan MX (2015) The endoplasmic reticulum stress sensor inositol-requiring enzyme 1alpha augments bacterial killing through sustained oxidant production. *MBio* 6: e00705

Ackerman AL, Kyritsis C, Tampe R, Cresswell P (2003) Early phagosomes in dendritic cells form a cellular compartment sufficient for cross presentation of exogenous antigens. *Proc Natl Acad Sci USA* 100: 12889 – 12894

Ackerman AL, Giodini A, Cresswell P (2006) A role for the endoplasmic reticulum protein retrotranslocation machinery during crosspresentation by dendritic cells. *Immunity* 25: 607 – 617

Alloatti A, Rookhuizen DC, Joannas L, Carpier JM, Iborra S, Magalhaes JG, Yatim N, Kozik P, Sancho D, Albert ML *et al* (2017) Critical role for Sec22b-dependent antigen cross-presentation in antitumor immunity. *J Exp Med* 214: 2231 – 2241

Arosa FA, Santos SG, Powis SJ (2007) Open conformers: the hidden face of MHC-I molecules. *Trends Immunol* 28: 115 – 123

Babdor J, Descamps D, Adiko AC, Tohme M, Maschalidi S, Evnouchidou I, Vasconcellos LR, De Luca M, Mauvais FX, Garfa-Traore M *et al* (2017) IRAP (+) endosomes restrict TLR9 activation and signaling. *Nat Immunol* 18: 509 – 518

Bachem A, Hartung E, Guttler S, Mora A, Zhou X, Hegemann A, Plantinga M, Mazzini E, Stoitzner P, Gurka S *et al* (2012) Expression of XCR1 characterizes the Batf3-dependent lineage of dendritic cells capable of antigen cross-presentation. *Front Immunol* 3: 214

Bachmair A, Finley D, Varshavsky A (1986) *In vivo* half-life of a protein is a function of its amino-terminal residue. *Science* 234: 179 – 186

Baravalle G, Schober D, Huber M, Bayer N, Murphy RF, Fuchs R (2005) Transferrin recycling and dextran transport to lysosomes is differentially affected by bafilomycin, nocodazole, and low temperature. *Cell Tissue Res* 320: 99 – 113

Basha G, Lizee G, Reinicke AT, Seipp RP, Omilusik KD, Jefferies WA (2008) MHC class I endosomal and lysosomal trafficking coincides with exogenous antigen loading in dendritic cells. *PLoS ONE* 3: e3247

Basha G, Omilusik K, Chavez-Steenbock A, Reinicke AT, Lack N, Choi KB, Jefferies WA (2012) A CD74-dependent MHC class I endolysosomal cross-presentation pathway. *Nat Immunol* 13: 237 – 245

Burgdorf S, Scholz C, Kautz A, Tampe R, Kurts C (2008) Spatial and mechanistic separation of cross-presentation and endogenous antigen presentation. *Nat Immunol* 9: 558 – 566

Campbell-Valois FX, Trost M, Chemali M, Dill BD, Laplante A, Duclos S, Sadeghi S, Rondeau C, Morrow IC, Bell C *et al* (2012) Quantitative proteomics reveals that only a subset of the endoplasmic reticulum contributes to the phagosome. *Mol Cell Proteomics* 11: M111 016378

Cebrian I, Visentin G, Blanchard N, Jouve M, Bobard A, Moita C, Enninga J, Moita LF, Amigorena S, Savina A (2011) Sec22b regulates phagosomal maturation and antigen crosspresentation by dendritic cells. *Cell* 147: 1355 – 1368

Chappell CP, Jacob J (2006) Identification of memory B cells using a novel transgenic mouse model. *J Immunol* 176: 4706 – 4715

Chen T, Han Y, Yang M, Zhang W, Li N, Wan T, Guo J, Cao X (2003) Rab39, a novel Golgi-associated Rab GTPase from human dendritic cells involved in cellular endocytosis. *Biochem Biophys Res Commun* 303: 1114 – 1120

Clipstone NA, Crabtree GR (1992) Identification of calcineurin as a key signalling enzyme in T-lymphocyte activation. *Nature* 357: 695 – 697

Cong L, Ran FA, Cox D, Lin S, Barretto R, Habib N, Hsu PD, Wu X, Jiang W, Marraffini LA *et al* (2013) Multiplex genome engineering using CRISPR/Cas systems. *Science* 339: 819 – 823

Cruz FM, Colbert JD, Merino E, Kriegsman BA, Rock KL (2017) The biology and underlying mechanisms of cross-presentation of exogenous antigens on MHC-I molecules. *Annu Rev Immunol* 35: 149 – 176

Deckhut AM, Allan W, McMickle A, Eichelberger M, Blackman MA, Doherty PC, Woodland DL (1993) Prominent usage of V beta 8.3 T cells in the H-2Db-restricted response to an influenza A virus nucleoprotein epitope. *J Immunol* 151: 2658 – 2666

Dudziak D, Kamphorst AO, Heidkamp GF, Buchholz VR, Trumpfheller C, Yamazaki S, Cheong C, Liu K, Lee HW, Park CG *et al* (2007) Differential antigen processing by dendritic cell subsets *in vivo*. *Science* 315: 107 – 111

van Endert P (2016) Intracellular recycling and cross-presentation by MHC class I molecules. *Immunol Rev* 272: 80 – 96

Fukuda M, Kanno E, Ishibashi K, Itoh T (2008) Large scale screening for novel rab effectors reveals unexpected broad Rab binding specificity. *Mol Cell Proteomics* 7: 1031 – 1042

Gambarte Tudela J, Capmany A, Romao M, Quintero C, Miserey-Lenkei S, Raposo G, Goud B, Damiani MT (2015) The late endocytic Rab39a GTPase regulates the interaction between multivesicular bodies and chlamydial inclusions. *J Cell Sci* 128: 3068 – 3081

Grant EP, Rock KL (1992) MHC class I-restricted presentation of exogenous antigen by thymic antigen-presenting cells *in vitro* and *in vivo*. *J Immunol* 148: 13 – 18

Guermonprez P, Saveanu L, Kleijmeer M, Davoust J, Van Endert P, Amigorena S (2003) ER-phagosome fusion defines an MHC class I cross-presentation compartment in dendritic cells. *Nature* 425: 397 – 402

Hansen TH, Lybarger L, Yu L, Mitaksov V, Fremont DH (2005) Recognition of open conformers of classical MHC by chaperones and monoclonal antibodies. *Immunol Rev* 207: 100 – 111

Harding CV, Song R (1994) Phagocytic processing of exogenous particulate antigens by macrophages for presentation by class I MHC molecules. *J Immunol* 153: 4925 – 4933

Hildner K, Edelson BT, Purtha WE, Diamond M, Matsushita H, Kohyama M, Calderon B, Schraml BU, Unanue ER, Diamond MS *et al* (2008) Batf3 deficiency reveals a critical role for CD8alpha+ dendritic cells in cytotoxic T cell immunity. *Science* 322: 1097 – 1100

Hochman JH, Jiang H, Matyus L, Edidin M, Pernis B (1991) Endocytosis and dissociation of class I MHC molecules labeled with fluorescent beta-2 microglobulin. *J Immunol* 146: 1862 – 1867

Hogquist KA, Jameson SC, Heath WR, Howard JL, Bevan MJ, Carbone FR (1994) T cell receptor antagonist peptides induce positive selection. *Cell* 76: 17 – 27

Hornung V, Bauernfeind F, Halle A, Samstad EO, Kono H, Rock KL, Fitzgerald KA, Latz E (2008) Silica crystals and aluminum salts activate the NALP3 inflammasome through phagosomal destabilization. *Nat Immunol* 9: 847 – 856

Houde M, Bertholet S, Gagnon E, Brunet S, Goyette G, Laplante A, Princiotta MF, Thibault P, Sacks D, Desjardins M (2003) Phagosomes are competent organelles for antigen cross-presentation. *Nature* 425: 402 – 406

Hsu PD, Scott DA, Weinstein JA, Ran FA, Konermann S, Agarwala V, Li Y, Fine EJ, Wu X, Shalem O *et al* (2013) DNA targeting specificity of RNA-guided Cas9 nucleases. *Nat Biotechnol* 31: 827 – 832

Huang AY, Golumbek P, Ahmadzadeh M, Jaffee E, Pardoll D, Levitsky H (1994) Role of bone marrow-derived cells in presenting MHC class I-restricted tumor antigens. *Science* 264: 961 – 965

Huang AY, Bruce AT, Pardoll DM, Levitsky HI (1996) *In vivo* cross-priming of MHC class I-restricted antigens requires the TAP transporter. *Immunity* 4: 349 – 355

Humphries W, Szymanski CJ, Payne CK (2011) Endo-lysosomal vesicles positive for Rab7 and LAMP1 are terminal vesicles for the transport of dextran. *PLoS ONE* 6: e26626

Johnson LS, Dunn KW, Pytowski B, McGraw TE (1993) Endosome acidification and receptor trafficking: bafilomycin A1 slows receptor externalization by a mechanism involving the receptor's internalization motif. *Mol Biol Cell* 4: 1251 – 1266

Jung S, Unutmaz D, Wong P, Sano G, De los Santos K, Sparwasser T, Wu S, Vuthoori S, Ko K, Zavala F *et al* (2002) *In vivo* depletion of CD11c+ dendritic cells abrogates priming of CD8+ T cells by exogenous cell-associated antigens. *Immunity* 17: 211 – 220

Kincaid EZ, Che JW, York I, Escobar H, Reyes-Vargas E, Delgado JC, Welsh RM, Karow ML, Murphy AJ, Valenzuela DM *et al* (2011) Mice completely lacking immunoproteasomes show major changes in antigen presentation. *Nat Immunol* 13: 129 – 135

Kovacsovics-Bankowski M, Clark K, Benacerraf B, Rock KL (1993) Efficient major histocompatibility complex class I presentation of exogenous antigen upon phagocytosis by macrophages. *Proc Natl Acad Sci USA* 90: 4942 – 4946

Kovacsovics-Bankowski M, Rock KL (1995) A phagosome-to-cytosol pathway for exogenous antigens presented on MHC class I molecules. *Science* 267: 243 – 246

Krzewski K, Gil-Krzewska A, Nguyen V, Peruzzi G, Coligan JE (2013) LAMP1/CD107a is required for efficient perforin delivery to lytic granules and NK-cell cytotoxicity. *Blood* 121: 4672 – 4683

Lawand M, Abramova A, Manceau V, Springer S, van Endert P (2016) TAP-dependent and -independent peptide import into dendritic cell phagosomes. *J Immunol* 197: 3454 – 3463

Lie WR, Myers NB, Connolly JM, Gorka J, Lee DR, Hansen TH (1991) The specific binding of peptide ligand to Ld class I major histocompatibility complex molecules determines their antigenic structure. *J Exp Med* 173: 449 – 459

Lizee G, Basha G, Tiong J, Julien JP, Tian M, Biron KE, Jefferies WA (2003) Control of dendritic cell cross-presentation by the major histocompatibility complex class I cytoplasmic domain. *Nat Immunol* 4: 1065 – 1073

Ljunggren HG, Stam NJ, Ohlen C, Neefjes JJ, Hoglund P, Heemels MT, Bastin J, Schumacher TN, Townsend A, Karre K *et al* (1990) Empty MHC class I molecules come out in the cold. *Nature* 346: 476 – 480

Mach N, Gillessen S, Wilson SB, Sheehan C, Mihm M, Dranoff G (2000) Differences in dendritic cells stimulated *in vivo* by tumors engineered to secrete granulocyte-macrophage colony-stimulating factor or Flt3-ligand. *Cancer Res* 60: 3239 – 3246

Mahmutefendic H, Blagojevic G, Kucic N, Lucin P (2007) Constitutive internalization of murine MHC class I molecules. *J Cell Physiol* 210: 445 – 455

Mahmutefendic H, Blagojevic G, Tomas MI, Kucic N, Lucin P (2011) Segregation of open major histocompatibility class I conformers at the plasma membrane and during endosomal trafficking reveals conformation-based sorting in the endosomal system. *Int J Biochem Cell Biol* 43: 504 – 515

Mahmutefendic H, Zagorac GB, Tomas MI, Groettrup M, Momburg F, Lucin P (2013) Endosomal trafficking of open major histocompatibility class I conformers–implications for presentation of endocytosed antigens. *Mol Immunol* 55: 149 – 152

Moore MW, Carbone FR, Bevan MJ (1988) Introduction of soluble protein into the class I pathway of antigen processing and presentation. *Cell* 54: 777 – 785

Mori Y, Matsui T, Omote D, Fukuda M (2013) Small GTPase Rab39A interacts with UACA and regulates the retinoic acid-induced neurite morphology of Neuro2A cells. *Biochem Biophys Res Commun* 435: 113 – 119

Nair-Gupta P, Baccarini A, Tung N, Seyffer F, Florey O, Huang Y, Banerjee M, Overholtzer M, Roche PA, Tampe R *et al* (2014) TLR signals induce phagosomal MHC-I delivery from the endosomal recycling compartment to allow cross-presentation. *Cell* 158: 506 – 521

Neefjes JJ, Momburg F, Hammerling GJ (1993) Selective and ATP-dependent translocation of peptides by the MHC-encoded transporter. *Science* 261: 769 – 771

Pfeifer JD, Wick MJ, Roberts RL, Findlay K, Normark SJ, Harding CV (1993) Phagocytic processing of bacterial antigens for class I MHC presentation to T cells. *Nature* 361: 359 – 362

Plovins A, Alvarez AM, Ibanez M, Molina M, Nombela C (1994) Use of fluorescein-di-beta-D-galactopyranoside (FDG) and C12-FDG as substrates for beta-galactosidase detection by flow cytometry in animal, bacterial, and yeast cells. *Appl Environ Microbiol* 60: 4638 – 4641

Rice J, Buchan S, Stevenson FK (2002) Critical components of a DNA fusion vaccine able to induce protective cytotoxic T cells against a single epitope of a tumor antigen. *J Immunol* 169: 3908 – 3913

Rock KL, Rothstein L, Gamble S (1990a) Generation of class I MHC-restricted T-T hybridomas. *J Immunol* 145: 804 – 811

Rock KL, Gamble S, Rothstein L (1990b) Presentation of exogenous antigen with class I major histocompatibility complex molecules. *Science* 249: 918 – 921

Rock KL, Gamble S, Rothstein L, Gramm C, Benacerraf B (1991) Dissociation of beta 2-microglobulin leads to the accumulation of a substantial pool of inactive class I MHC heavy chains on the cell surface. *Cell* 65: 611 – 620

Rock KL, Rothstein L, Gamble S, Fleischacker C (1993) Characterization of antigen-presenting cells that present exogenous antigens in association with class I MHC molecules. *J Immunol* 150: 438 – 446

Rock KL, Gramm C, Rothstein L, Clark K, Stein R, Dick L, Hwang D, Goldberg AL (1994) Inhibitors of the proteasome block the degradation of most cell proteins and the generation of peptides presented on MHC class I molecules. *Cell* 78: 761 – 771

Saveanu L, Carroll O, Weimershaus M, Guermonprez P, Firat E, Lindo V, Greer F, Davoust J, Kratzer R, Keller SR *et al* (2009) IRAP identifies an endosomal compartment required for MHC class I cross-presentation. *Science* 325: 213 – 217

Savina A, Jancic C, Hugues S, Guermonprez P, Vargas P, Moura IC, Lennon-Dumenil AM, Seabra MC, Raposo G, Amigorena S (2006) NOX2 controls phagosomal pH to regulate antigen processing during crosspresentation by dendritic cells. *Cell* 126: 205 – 218

Serwold T, Gonzalez F, Kim J, Jacob R, Shastri N (2002) ERAAP customizes peptides for MHC class I molecules in the endoplasmic reticulum. *Nature* 419: 480 – 483

Shen Z, Reznikoff G, Dranoff G, Rock KL (1997) Cloned dendritic cells can present exogenous antigens on both MHC class I and class II molecules. *J Immunol* 158: 2723 – 2730

Shen L, Rock KL (2004) Cellular protein is the source of cross-priming antigen *in vivo*. *Proc Natl Acad Sci USA* 101: 3035 – 3040

Shen L, Sigal LJ, Boes M, Rock KL (2004) Important role of cathepsin S in generating peptides for TAP-independent MHC class I crosspresentation *in vivo*. *Immunity* 21: 155 – 165

Seto S, Tsujimura K, Koide Y (2011) Rab GTPases regulating phagosome maturation are differentially recruited to mycobacterial phagosomes. *Traffic* 12: 407 – 420

Seto S, Sugaya K, Tsujimura K, Nagata T, Horii T, Koide Y (2013) Rab39a interacts with phosphatidylinositol 3-kinase and negatively regulates autophagy induced by lipopolysaccharide stimulation in macrophages. *PLoS ONE* 8: e83324

Sigal LJ, Crotty S, Andino R, Rock KL (1999) Cytotoxic T-cell immunity to virus-infected non-haematopoietic cells requires presentation of exogenous antigen. *Nature* 398: 77 – 80

Singh R, Cresswell P (2010) Defective cross-presentation of viral antigens in GILT-free mice. *Science* 328: 1394 – 1398

Stenmark H (2009) Rab GTPases as coordinators of vesicle traffic. *Nat Rev Mol Cell Biol* 10: 513 – 525

Sugita M, Brenner MB (1995) Association of the invariant chain with major histocompatibility complex class I molecules directs trafficking to endocytic compartments. *J Biol Chem* 270: 1443 – 1448

Towne CF, York IA, Watkin LB, Lazo JS, Rock KL (2007) Analysis of the role of bleomycin hydrolase in antigen presentation and the generation of CD8 T cell responses. *J Immunol* 178: 6923 – 6930

Trost M, English L, Lemieux S, Courcelles M, Desjardins M, Thibault P (2009) The phagosomal proteome in interferon-gamma-activated macrophages. *Immunity* 30: 143 – 154

Tse DB, Cantor CR, McDowell J, Pernis B (1986) Recycling class I MHC antigens: dynamics of internalization, acidification, and ligand-degradation in murine T lymphoblasts. *J Mol Cell Immunol* 2: 315 – 329

Vigna JL, Smith KD, Lutz CT (1996) Invariant chain association with MHC class I: preference for HLA class I/beta 2-microglobulin heterodimers, specificity, and influence of the MHC peptide-binding groove. *J Immunol* 157: 4503 – 4510

Wearsch PA, Cresswell P (2008) The quality control of MHC class I peptide loading. *Curr Opin Cell Biol* 20: 624 – 631

van Weering JR, Toonen RF, Verhage M (2007) The role of Rab3a in secretory vesicle docking requires association/dissociation of guanidine phosphates and Munc18-1. *PLoS ONE* 2: e616

Weigert R, Yeung AC, Li J, Donaldson JG (2004) Rab22a regulates the recycling of membrane proteins internalized independently of clathrin. *Mol Biol Cell* 15: 3758 – 3770

Weimershaus M, Maschalidi S, Sepulveda F, Manoury B, van Endert P, Saveanu L (2012) Conventional dendritic cells require IRAP-Rab14 endosomes for efficient cross-presentation. *J Immunol* 188: 1840 – 1846

Wu SJ, Niknafs YS, Kim SH, Oravecz-Wilson K, Zajac C, Toubai T, Sun Y, Prasad J, Peltier D, Fujiwara H *et al* (2017) A critical analysis of the role of SNARE protein SEC22B in antigen cross-presentation. *Cell Rep* 19: 2645 – 2656

York IA, Chang SC, Saric T, Keys JA, Favreau JM, Goldberg AL, Rock KL (2002) The ER aminopeptidase ERAP1 enhances or limits antigen presentation by trimming epitopes to 8-9 residues. *Nat Immunol* 3: 1177 – 1184

York IA, Bhutani N, Zendzian S, Goldberg AL, Rock KL (2006) Tripeptidyl peptidase II is the major peptidase needed to trim long antigenic precursors, but is not required for most MHC class I antigen presentation. *J Immunol* 177: 1434 – 1443

Yu YY, Myers NB, Hilbert CM, Harris MR, Balendiran GK, Hansen TH (1999) Definition and transfer of a serological epitope specific for peptide-empty forms of MHC class I. *Int Immunol* 11: 1897 – 1906

Zehner M, Marschall AL, Bos E, Schloetel JG, Kreer C, Fehrenschild D, Limmer A, Ossendorp F, Lang T, Koster AJ *et al* (2015) The translocon protein Sec61 mediates antigen transport from endosomes in the cytosol for cross-presentation to CD8(+) T cells. *Immunity* 42: 850 – 863